General Disclaimer

One or more of the Following Statements may affect this Document

- This document has been reproduced from the best copy furnished by the organizational source. It is being released in the interest of making available as much information as possible.

- This document may contain data, which exceeds the sheet parameters. It was furnished in this condition by the organizational source and is the best copy available.

- This document may contain tone-on-tone or color graphs, charts and/or pictures, which have been reproduced in black and white.

- This document is paginated as submitted by the original source.

- Portions of this document are not fully legible due to the historical nature of some of the material. However, it is the best reproduction available from the original submission.

9950-828

FINAL TECHNICAL REPORT
October 1982

Title: Nondestructive Evaluation Techniques for Nickel-Cadmium Aerospace Battery Cells

Contract Number:	955708
Contract Period:	April 1980 - September 1982
Contractor:	Rockwell International Corporation Microelectronics Research and Development Center Thousand Oaks, CA 91360
Authors:	Ron Haak and Dennis Tench
Document Number:	MRDC41057.63FR
Sponsored by:	Jet Propulsion Laboratory Pasadena, CA 91103
Task Order Number:	RD-156

This work was performed for the Jet Propulsion Laboratory, California Institute of Technology sponsored by the National Aeronautics and Space Administration under Contract NA67-918.

TABLE OF CONTENTS

LIST OF FIGURES

LIST OF FIGURES

LIST OF TABLES

1.0 ABSTRACT

The goal of the project was to evaluate the ac impedance characteristics of Ni-Cd cells as an in-situ, non-destructive means of determining cell lifetime, particularly with respect to the probability of premature failure. Emphasis of the program was on evaluating Ni-Cd cell impedance over a wide frequency range (10,000 to 0.0004 Hz) as the cells were subjected to charge/discharge cycle testing.

The results indicate that cell degradation is reflected in the low frequency (Warburg) impedance characteristics associated with diffusion processes. The Warburg slope (W) was found to steadily increase as a function of cell aging for completely discharged cells. In addition, based on data for two cells, a high or rapidly increasing value for W signals imminent cell failure by one mechanism. Degradation by another mechanism is apparently reflected in a fall-off (roll-over) of W at lower frequencies.

As a secondary result, the frequency dependence of the absolute cell impedance at low frequencies (5 - 500 mHz) was found to be a good indication of the cell state-of-charge.

2.0 INTRODUCTION AND BACKGROUND

2.1 Rationale and Overall Approach

The overall objective of this program was to develop a non-destructive method for predicting the cycle life of Ni-Cd batteries. The approach taken was based on ac impedance measurements, which, because of the cyclic nature of the perturbation involved, would be expected to be particularly sensitive to the irreversibilities in the electrode reactions that ultimately lead to battery failure. Although there are inherent irreversibilities in the electrode processes which limit the attainable cycle life, the present effort was focused on detecting flaws which enhance/introduce irreversibilities that lead to premature failure.

Irreversible processes of interest would be expected to generally involve mobile reactant species, primarily ions in solutions and adions in the electrode surface, which can segregate and lead to densification, dendritic growth, and loss of active material. The electrode flaws that are likely to enhance these detrimental processes include crystalline imperfections, impurity centers, and surface irregularities. As an example, Cd ions and/or adions may deposit preferentially at lattice dislocation sites and then not totally redissolve or disperse during discharge of the battery because of the additional binding energy associated with the dislocations. If the amount of segregated material increases with battery cycling, dendrites will form which may ultimately penetrate the separator and short the cell. For convenience, we will use the term "fatal" flaw to refer to the particular flaw which ultimately leads to battery failure.

The probability that the existence of fatal flaws can be ascertained from ac impedance measurements early in the cycle life of the battery would depend on whether such flaws occur as isolated events or statistically in conjunction with more benign flaws. Using the example from the preceding paragraph, we might imagine that any lattice dislocation of a particular type in the electrode material would lead to a dendrite which ultimately penetrates

the separator and shorts the cell. Such isolated flaws would be extremely difficult to detect in the early life of the battery because they would represent such a small portion of the active electrode material. Fortunately, it is unlikely that such isolated flaws are responsible for most premature battery failures since flaws, e.g., dendrites, are generally found in large numbers in healthy cells which have delivered the normal number of cycles. It is more probable that "fatal" flaws are slight variations of benign flaws and are simply more likely to occur when the flaw density is high. For instance, in our example above, a fatal flaw might be a particularly severe or twinned lattice dislocation, or a dislocation which occurs in the vicinity of a flaw in the separator material.

In such cases, the probability that a fatal flaw exists would be expected to increase with the overall density of flaws of a given type. Thus, one could reasonably expect to relate battery cycle life to the densities of flaws, which should be detectable by ac impedance measurements via the associated irreversibilities in the electrode reactions.

In the present program, the approach was to monitor the ac impedance characteristics of Ni-Cd cells as they were subjected to charge/discharge cycle testing. The principal test conditions involved various depths of discharge and various temperatures. Ideally, a given cell would be characterized prior to cycling and at close intervals during the test program to permit ac impedance parameters to be correlated with increased flaw density/premature failure.

2.2 AC Impedance Method/Previous Work

Since most electrochemical systems can be represented by series and parallel combinations of various electronic circuit elements, the analysis of ac impedance data usually involves construction of "equivalent circuits" which provide a model for understanding the chemical and electrochemical processes occurring. For example, a typical electrochemical interface can be represented by the equivalent circuit shown in Fig. 1, where R_S is the sum of

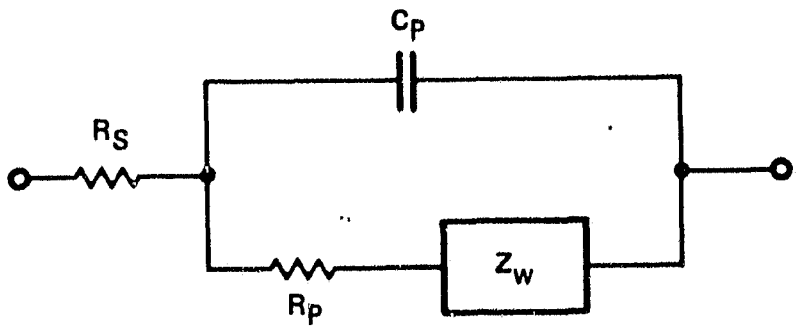

Fig. 1 Equivalent circuit for a simple electrochemical interface.

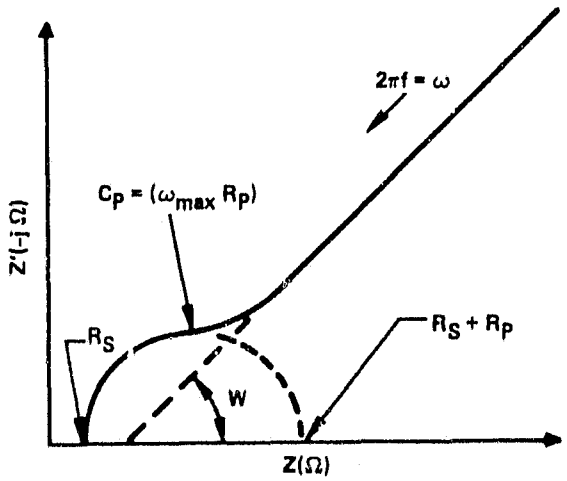

Fig. 2 Impedance spectrum for the equivalent circuit of Fig. 1 measured over an extended frequency range.

solution, separator and lead ohmic resistances, C_p is the parallel capacitance which is usually dominated by the double layer capacitance (C_{DL}), R_p is the parallel resistance which is usually dominated by the charge transfer resistance (R_{CT}), and Z_W is the diffusional (Warburg) impedance. In simple cases, the values of the various circuit elements can be determined by plotting the real (Z') and imaginary (Z") components of the impedance for a wide range of perturbation frequencies. Such a complex plane plot, with the circuit elements labeled, is shown in Fig. 2.

The relevance of these elements to the present work can be appreciated by considering their physical significance. Ohmic resistance (R_s) is primarily associated with the electrolyte and separator, and should reflect dewetting or deterioration of the separator, migration of active material into the separator, and perhaps increased plate surface resistance. The double layer capacitance (C_{DL}) is associated with charge separation across the interface, and depends on the electrode surface area and concentrations of ions, adions and adsorbed species. Through C_{DL}, it may be possible to detect very small concentrations of flaws from the effect that they exert on the concentration of charged intermediates, e.g., adions. In addition, C_{DL} should be sensitive to active surface area variations associated with densification, expansion of plates, or pore blockage. Charge transfer resistance (R_{CT}) is determined by the rate of electrochemical reactions. Low values of R_{CT} might signal abnormal plate growth corresponding to agglomeration of active material with possible dendrite formation. High values of R_{CT} could reflect irreversible reactions associated with crystal formation or other losses of active material. Diffusional impedance (Z_W) arises at low frequencies where many reactions are diffusion controlled. The Warburg coefficient, determined from the diffusion impedance, provides a measure of the surface concentrations of reaction intermediates (adions) and might, therefore, be used to detect surface flaws. In addition, the variation in Z_W with signal frequency depends on the electrode porosity and may reflect electrode densification or pore blockage.

To simplify analysis of results obtained from the more complicated systems, data are often plotted in various alternate forms which permit a more precise determination of the various equivalent circuit features. Log-log plots of the total impedance (Z) and the real (Z') and imaginary (Z") components vs frequency can be particularly useful. Such plots for the equivalent circuit in Fig. 1 are depicted in Fig. 3. The Warburg coefficient, σ, which is an important diffusional parameter, is obtained from plots of Z' or Z" vs ω^{χ} over frequency regions where diffusion control predominates, where χ is a coefficient which reflects the morphology of the electrode (e.g., $\chi = 1/2$ for a planar electrode and 1/4 for an ideal porous electrode). If the electrode morphology is unknown, the value of χ can be obtained from log-log plots of Z' or Z" vs ω.

The equivalent circuit for Ni-Cd cells, which consist of two electrodes electrically connected in series via an electrolyte/separator, is considerably more complex than the circuit in Fig. 1. In addition, inductive circuit elements may also be present, and the values of the various in-phase resistive components can be frequency dependent. The situation is further complicated by the fact that the cell electrodes are porous.

Impedance characteristics of porous electrodes have been treated theoretically by De Levie [1], using a transmission line model and assuming infinitely-deep cylindrical pores of uniform cross section. Whereas interfacial impedances are simply additive for a planar surface, they combine as the geometric mean for such porous electrodes. Consequently, impedance characteristics for a given process may be significantly affected by the electrode porosity. For example, whereas the diffusional impedance for a planar electrode is directly proportional to $\omega^{-1/2}$ (ω = perturbation frequency), it is proportional to $\omega^{-1/4}$ for porous electrodes of the type treated by De Levie. For electrodes having such idealized pores, the impedance can be correlated with that for planar electrodes by squaring the absolute magnitude of the impedance and doubling the phase angle [1].

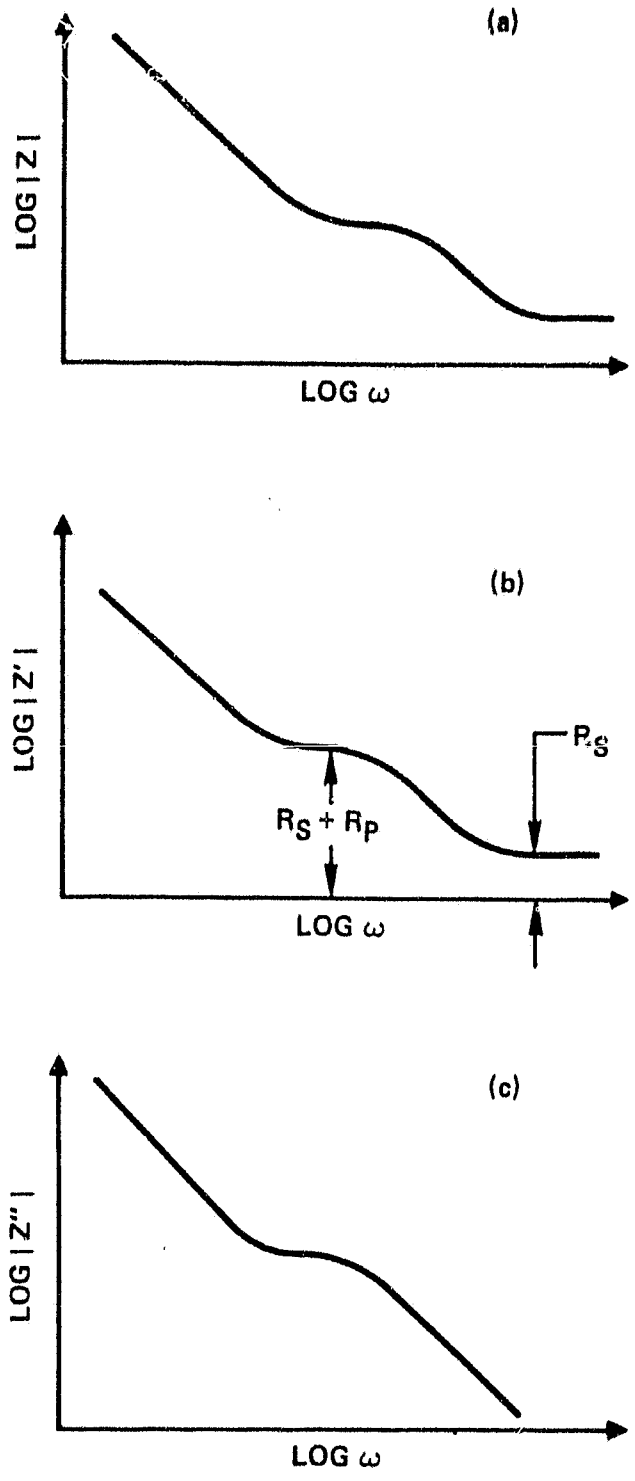

Fig. 3 Plotting methods for treating ac impedance data.

For real porous electrode systems, nonidealized behavior must also be considered. For example, since at lower perturbation frequencies pores must be deeper to behave as though infinitely deep, a transition from porous to nonporous electrode behavior can occur as ω is changed over a few decades [1]. Thus, for a typical frequency scan, which covers seven decades (e.g., 10 kHz to 1 mHz), it is quite possible to encounter both porous and nonporous behavior. This effect has been used to advantage by Armstrong et al. [2], who were able to detect a decrease in pore length for Cd electrodes in alkaline solution, caused by redistribution of active material and a progressive build-up of $Cd(OH)_2$ during charge/discharge cycling. The effect of pore geometry on impedance spectra has been addressed by Keiser et al. [3]; noncylindrical pores, especially those with occluded geometries, were shown to exhibit anamalous impedance behavior. These authors were able to discern the average pore structure of a nickel electrode from impedance studies.

For actual commercial cells, these are additional difficulties associated with the impedance measurement itself. Since the cell is typically sealed, only the impedance of the total cell can be measured, and the contributions of the individual electrodes and electrolyte/separator must be inferred subsequently. Also, because of the large charge capacity of many commercial batteries, a compromise in the magnitude of the perturbation signal is often required; even a 1 mV signal can yield current responses in the 1 A range (which are difficult to handle electronically), whereas the signal to noise ratio may be poor for smaller perturbations.

In spite of the difficulties involved, the impedance characteristics of several commercial battery systems have recently been investigated, typically with the goal of developing a method for determining the state-of-charge. Hampson, et al. [4] have reviewed the literature prior to 1979 and developed a general theory for describing the impedance of batteries. Systems that have been studied, most of them in the last three years, include Zn/HgO [5,6], Zn/MnO_2 [7,8], Leclanche' cells [9-11], Pb/H_2SO_4 [12-14], Mg/MnO_2 [8], and Ni-Cd [15,16]. The effect of charge/discharge cycling on

Pb [17] and sintered-plate Cd [2] electrodes have also been investigated. These studies, although not particularly successful in establishing state-of-charge correlations, have demonstrated the value of ac impedance for investigation of battery properties.

As described by Pilla [18], impedance characteristics can also be determined by the analysis of current transients, and the results can be converted from the time domain to the frequency domain using Laplace transformations. Zimmerman, et al. used the transient technique to study the impedance of 10 A-hr sintered-plate Ni-Cd cells at equivalent ac frequencies from 10 to 0.1 mHz, and the ac method at higher frequencies. Most of the information pertaining to diffusional and film growth processes is obtained in this low frequency range, which had not been previously investigated.

Results obtained for Ni-Cd cells are of particular relevance to the present work. Zimmerman and his co-workers [15] showed that the impedance of an operating Ni-Cd battery is dominated by mass transport processes. Two diffusional features were observed in the impedance spectra: one apparently corresponding solid state proton diffusion within the nickel oxy-hydroxide electrode and the other to cadmium diffusion. A finding which would tend to validate the approach taken in the present program was that the diffusional processes in Ni-Cd cells are sensitive to changes in the morphology or chemical structure of the electrode active material. These workers also found that the inductive impedance observed above 10 Hz was insensitive to the cell state-of-charge and the current, and could be attributed to self-inductance of current collection leads and assemblies. Sathyanarayana, et al. [16], using an ac technique from 5-30 Hz, also found that the impedance of Ni-Cd cells is dominated by diffusion and may be interpreted in terms of a long cylindrical pore model. The latter authors found that the equivalent series or parallel capacitance reflected (within 20-30%) the battery's state-of-charge.

3.0 TECHNICAL RESULTS

This program was focused on developing a non-destructive ac impedance method for predicting the cycle life of Ni-Cd aerospace cells. The overall approach was to monitor the ac impedance characteristics of cells subjected to cycle testing at JPL, and to correlate impedance parameters with cycle life.

3.1 Experimental Details

Testing was performed on 12 A-hr sealed cells (General Electric) for which the Ni active material was either chemically (L2 series) or electrochemically (L1 series) deposited. The charge/discharge cycle was based on a satellite low earth orbit and consisted of 60 minutes charging and 40 minutes discharging. Nine test conditions were used, defined by the matrix of three temperatures (20, 30 and 40°C) and three depths of discharge (20, 35 and 50%). Statistical information is available for the average cycle life under a given set of conditions; for example, at 40°C and 50% depth of discharge, cells have a 63% chance of failing by 3100 cycles.

A block diagram of the apparatus used for ac impedance measurements is shown in Fig. 4. The heart of the system is a Solartron Model 1172 frequency response analyzer which determines the real and imaginary components of the impedance as a function of frequency by impressing a small voltage across the cell (via the potentiostat) and analyzing the current response. The voltage perturbation used in the present work was 2 mV (rms), except for preliminary studies (10 mV). Impedance was measured from 10 kHz to about 0.4 mHz, with 20 logarithmically-spaced points per decade of frequency. Full computer control of the experiments and data handling was provided by a Hewlett-Packard Model 9825 desktop computer. The potentiostat used (Stonehard Model BC1200) has the advantage of dual reference inputs (see Fig. 4), which minimize lead wire inductive effects - an important feature in view of the high current responses involved.

Typically, cells were first discharged at the C/20 rate (~ 600 mA) to 0.00 V, and the impedance spectrum was determined for the totally discharged

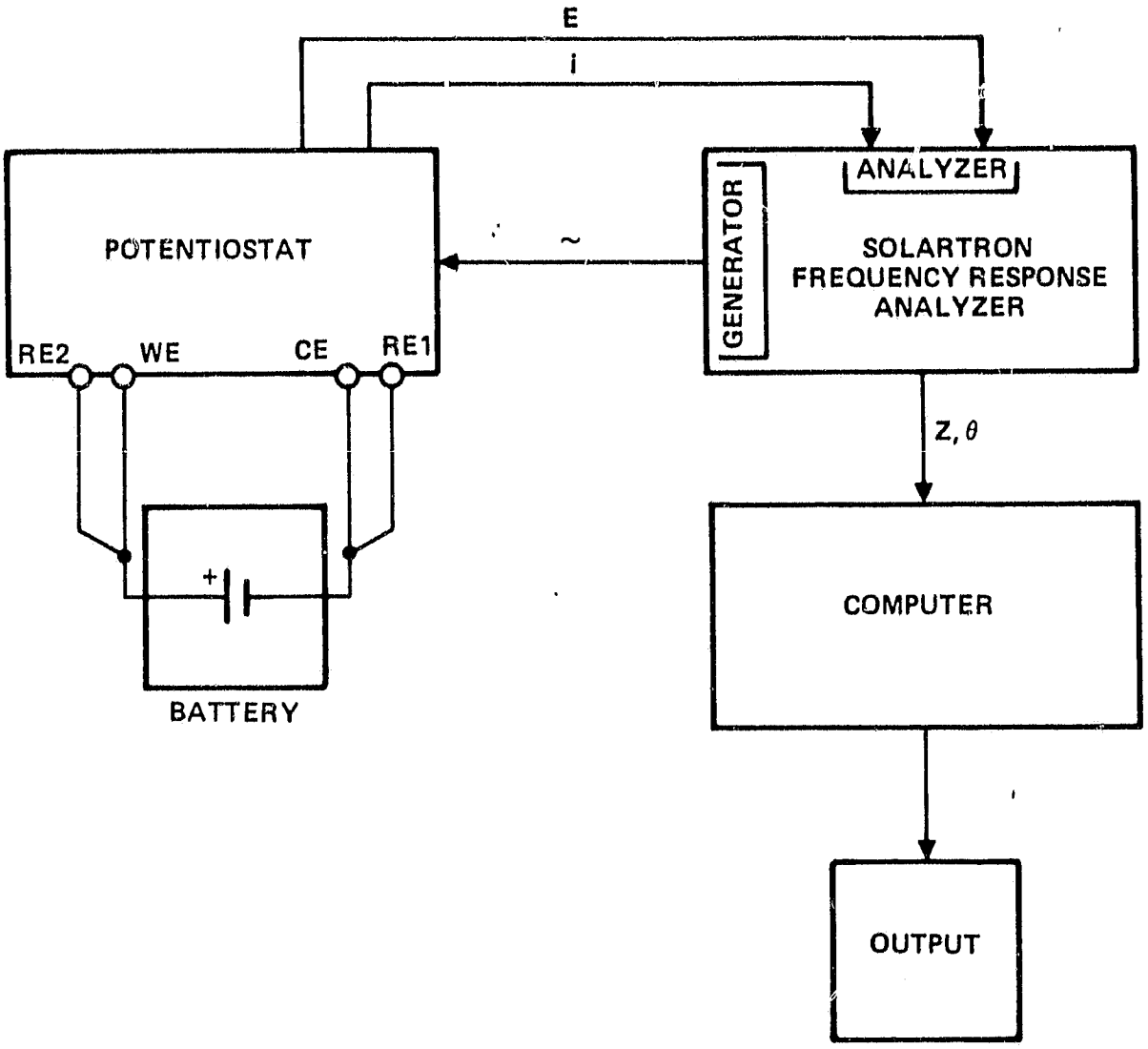

Fig. 4. Block diagram of the ac impedance measurement system.

state. In some cases, impedance measurements were also made at various other states-of-charge. Some experiments were performed under galvanostatic rather than potentiostatic control.

3.2 Preliminary Studies

Initial studies involved 12 cells, nine of which had undergone charge/discharge cycling, and were directed toward establishing suitable measurement conditions (charge state, frequency range, integration time and perturbation magnitude) and baseline data for subsequent comparisons. Impedance spectra were measured, using a 10 mV (rms) voltage perturbation, for various states of change, i.e., totally discharged (0.0 V), slightly charged (1.0 V), and with 4, 8 and 12 A-hr of charge.

At frequencies greater than about 10 Hz for charged cells and 100 Hz for those totally discharged, the impedance is apparently dominated by inductance associated with the electrical leads. This was demonstrated by measuring the impedance of isolated resistors (0.02, 0.05 and 0.1 ohm) chosen to simulate the Ni-Cd cells; an inductive response similar to that obtained for the cells was observed. Because of these results, which are in agreement with those reported in the literature [15], the inductive portions of impedance spectra were ignored and are not reported here.

Representative impedance data plotted in the complex plane* for two cells at various states of charge are shown in Figs. 5 - 8. In interpreting these data, it is instructive to consider the overall electrode reactions, i.e.,

$$NiOOH + H_2O + e^- \underset{\text{charge}}{\overset{\text{discharge}}{\rightleftharpoons}} OH^- + Ni(OH)_2 \qquad (1)$$

$$Cd + 2OH^- \underset{\text{charge}}{\overset{\text{discharge}}{\rightleftharpoons}} 2e^- + Cd(OH)_2 \qquad 2)$$

*Data were plotted in various other ways but only complex plane plots are discussed in this section.

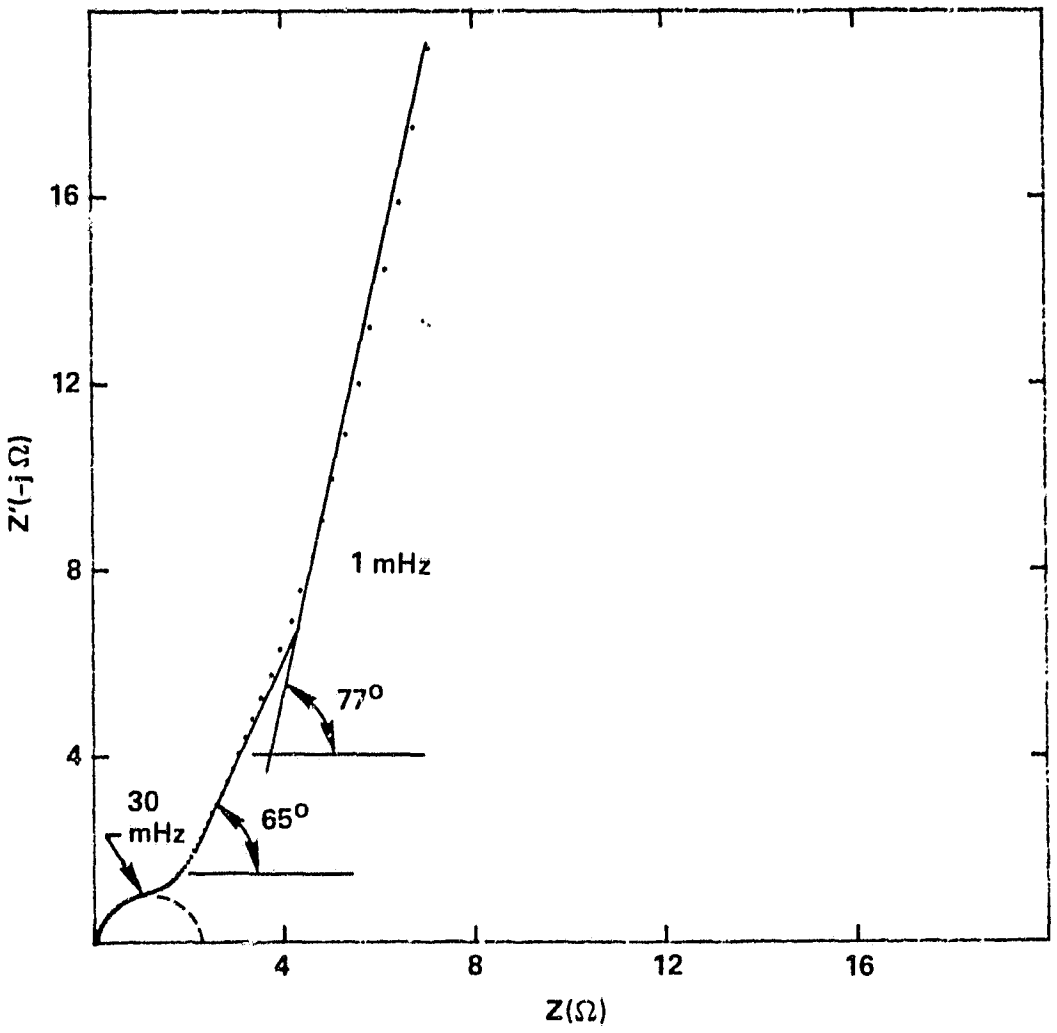

Fig. 5 Complex impedance spectrum for Ni-Cd cell L2-82 at 0.0 V (fully discharged).

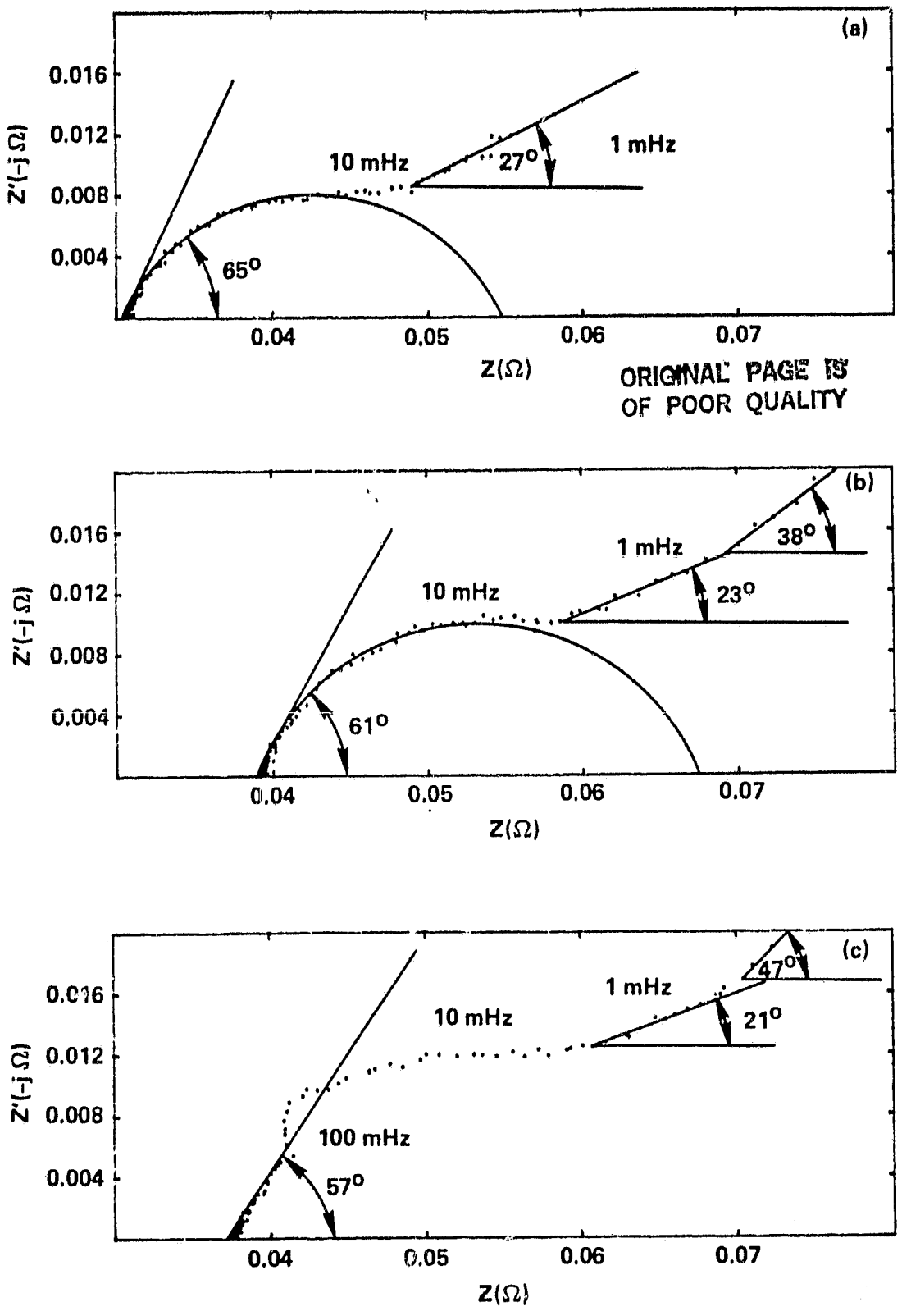

Fig. 6 Complex impedance spectra for Ni-Cd cell L2-82 at charge states of: (a) 4, (b) 8 and (c) 12 A-hr.

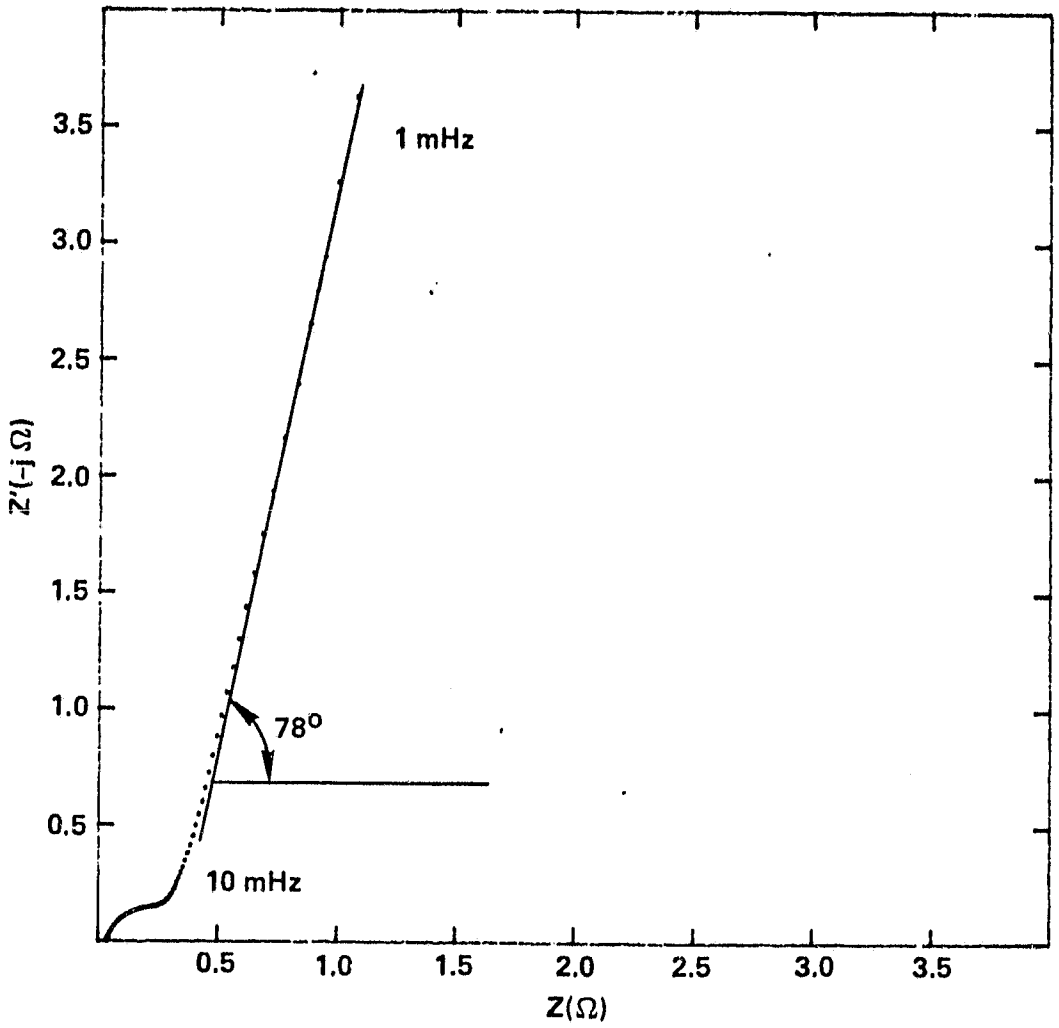

Fig. 7 Complex impedance spectrum for Ni-Cd cell L2-92 at 0.0 V (fully discharged).

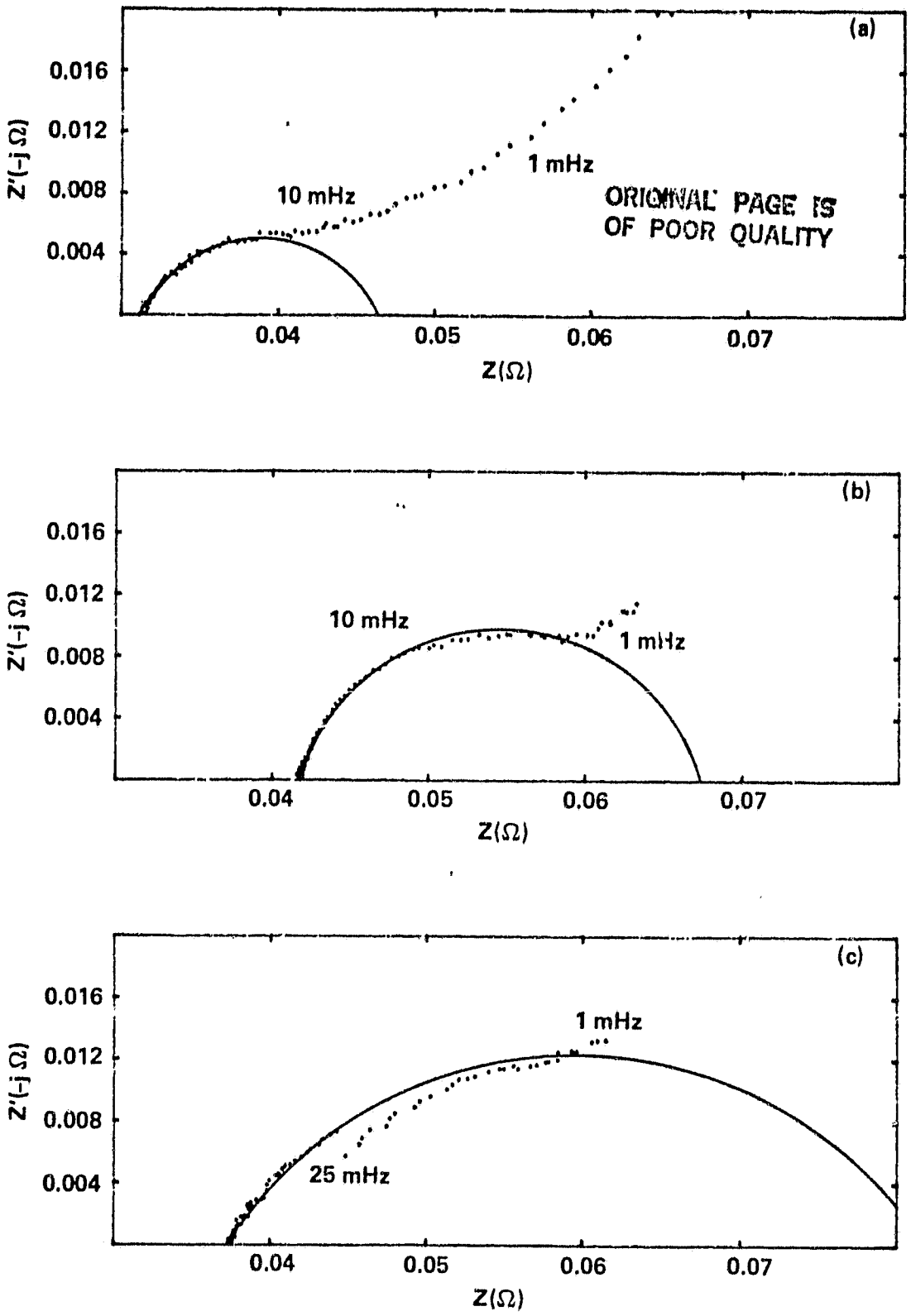

Fig. 8 Complex impedance spectra for Ni-Cd cell L2-92 at charge states of: (a) 4, (b) 8 and (c) 12 A-hr.

Since Ni-Cd cells are typically constructed with excess negative (Cd) electrode capacity, the cell impedance for the totally discharged state (Figs. 5 and 7) is dominated by the Ni electrode. Note that the overall impedance is relatively high, probably because of the presence of a resistive nickel hydroxide layer. In this case, the equivalent circuit given in Fig. 1 is at least approximately applicable. However, the low frequency slopes are considerably greater (65-80°) than expected for a diffusional process to either a planar electrode (45°) or a porous electrode (22°). Such large slopes are probably associated with pore shape, solid-state diffusion or slow adsorption/desorption processes (perhaps involving protons). Since the electrode processes involved are unknown, circuit elements are given the more general designations, R_p and C_p, rather than R_{CT} and C_{DL}.

For partially or fully charged cells, the impedance behavior is more complex (Figs. 6 and 8). Although well-defined semicircles are generally observed for the lower states of charge, the diffusional impedance region is often non-linear (see Fig. 8a), which makes it difficult to tabulate data and make quantitative comparisons. Nonetheless, note that the diffusional slopes tend to fall in the range expected for a porous electrode (20 - 40°). Interestingly, for the highest state of charge (12 A-hr), an inflection in the impedance spectrum is often observed at a Z' value of about 0.42 Ω (see Figs. 6c and 8c).

Because of the limited resources available for this program, it was necessary to limit measurements to either a few cells or one charge state. It was decided to monitor the impedance characteristics of the maximum number of cells at one state of charge so as to maximize the probability of including cells that would fail prematurely; such cells are essential to establishing definite correlations between ac impedance parameters and cell cycle life. The fully discharged state, for which a relatively simple equivalent circuit model appears to be applicable, was chosen. This choice also facilitates data acquisition since the zero charge state can be reproducibly attained and measurement problems associated with high current response are minimized (cell resistance is largest). Based on these preliminary studies, a perturbation voltage of 2 mV (rms) was also selected.

3.3 Failure Prediction

AC impedance data were determined (as a function of frequency) for Ni-Cd cells (in the fully discharged state) at various points during charge discharge cycle testing and were routinely plotted in the four ways illustrated in Figs. 9 - 12. From the complex plane plots (Fig. 9), R_p, C_p and W (see Section 2.1) were determined (whenever possible) and tabulated.* Log-log plots of the total impedance (Z) and its imaginary (Z'') and real (Z') components vs frequency (ω) generally exhibited two linear regions. The slopes and inflection points for such plots were also tabulated, using the notation given in Figs. 10 - 12. Data tabulations for all cells evaluated are given in the Appendix.

Data for the impedance parameters found to depend on the cell charge/discharge history, i.e., W and C_p, are summarized in Table I. For both types of cells (Ni active material chemically deposited for L2 series and electrodeposited for L1 series), W increases steadily with the number of charge/discharge cycles after the initial conditioning period.† Interestingly, C_p decreases with cycling for L2 cells but increases for L1 cells.

Based on data for two cells, a high or rapidly increasing value for W apparently signals imminent cell failure. This is most evident for cell L2-95 which yielded a W value of 87.1° when evaluated at 3124 cycles (Table I) and failed only 200 cycles later; note that W typically falls in the 60-75° range. The complex impedance spectrum for this cell is shown in Fig. 13. Likewise, W for cell L2-68 steadily increased and was high (82.1°) when evaluated at 5223 cycles, just before failure. Unfortunately, only four of the cells monitored by ac impedance failed during the course of this work so that a firm correlation between W and cell failure could not be established. It should be mentioned, however, that high W values have been reported [10] for Leclanche' cells and attributed to polarization of the carbon electrode caused by inadequate sorptive or electrocatalytic properties.

---

*Note that R_s was neglected since it was found to be insensitive to the battery charge state and cycling history.

†Note that Ni-Cd cells typically must undergo several charge/discharge cycles before normal behavior is obtained.

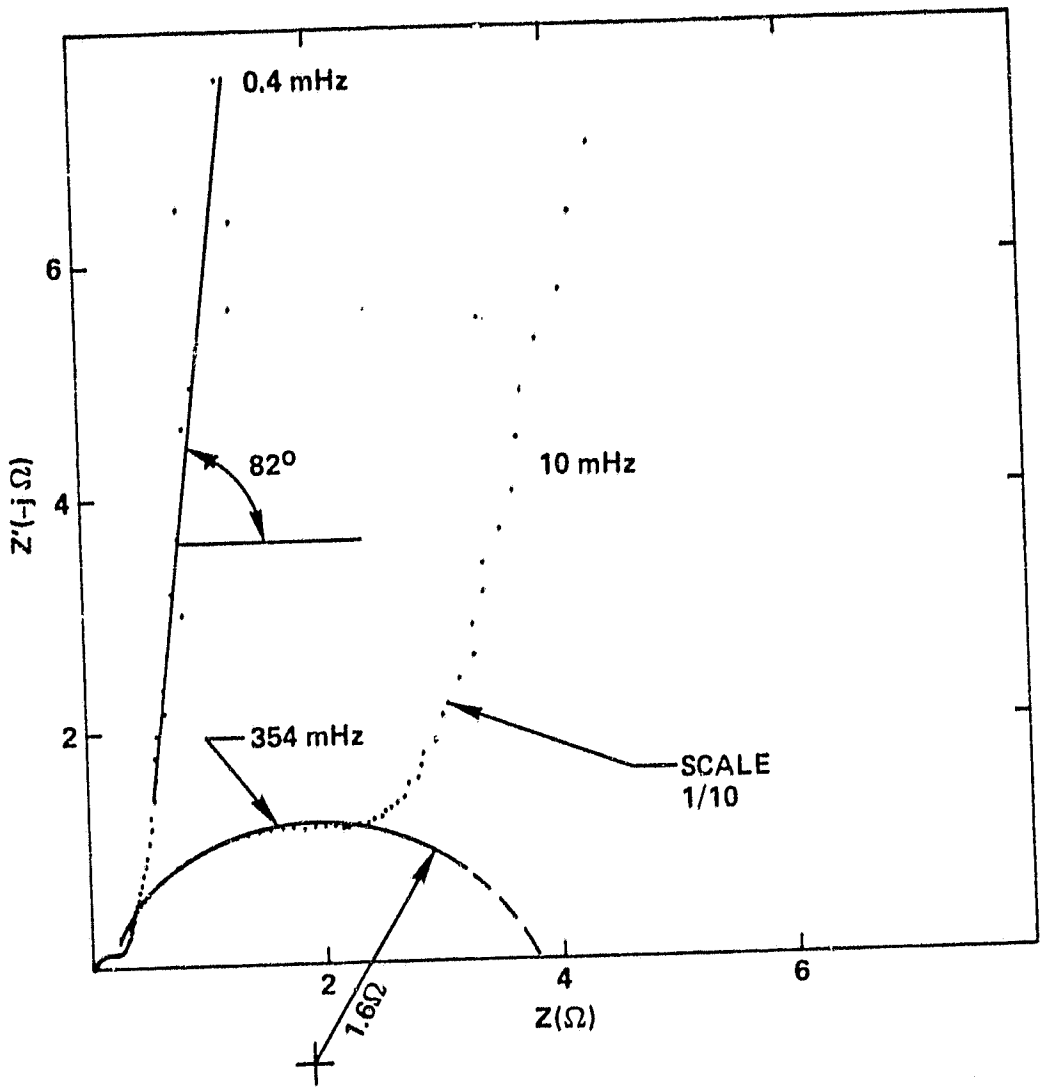

Fig. 9 Complex impedance spectrum for Ni-Cd cell L2-59 at 0.0 V after 3457 charge/discharge cycles.

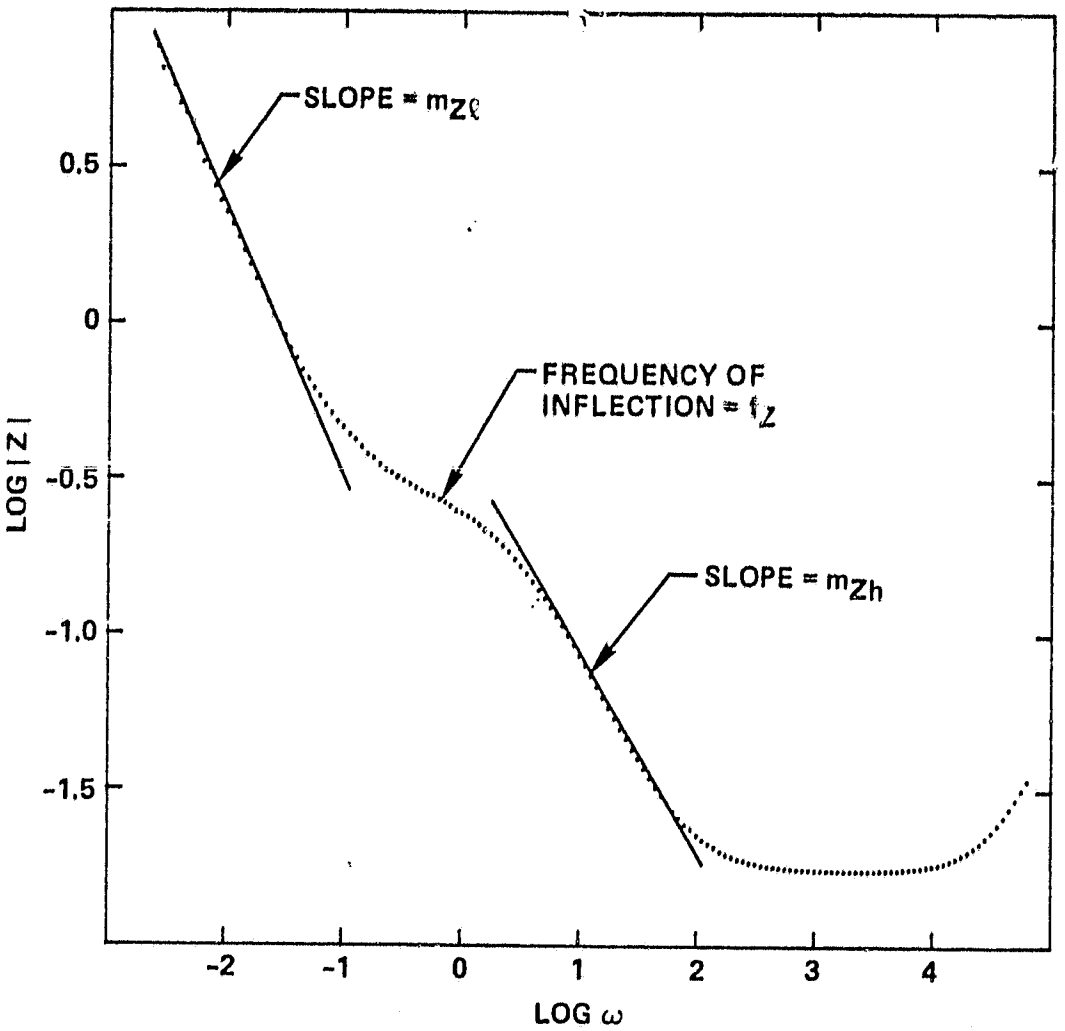

Fig. 10 Log-log plot of total impedance vs frequency for the data given in Fig. 9.

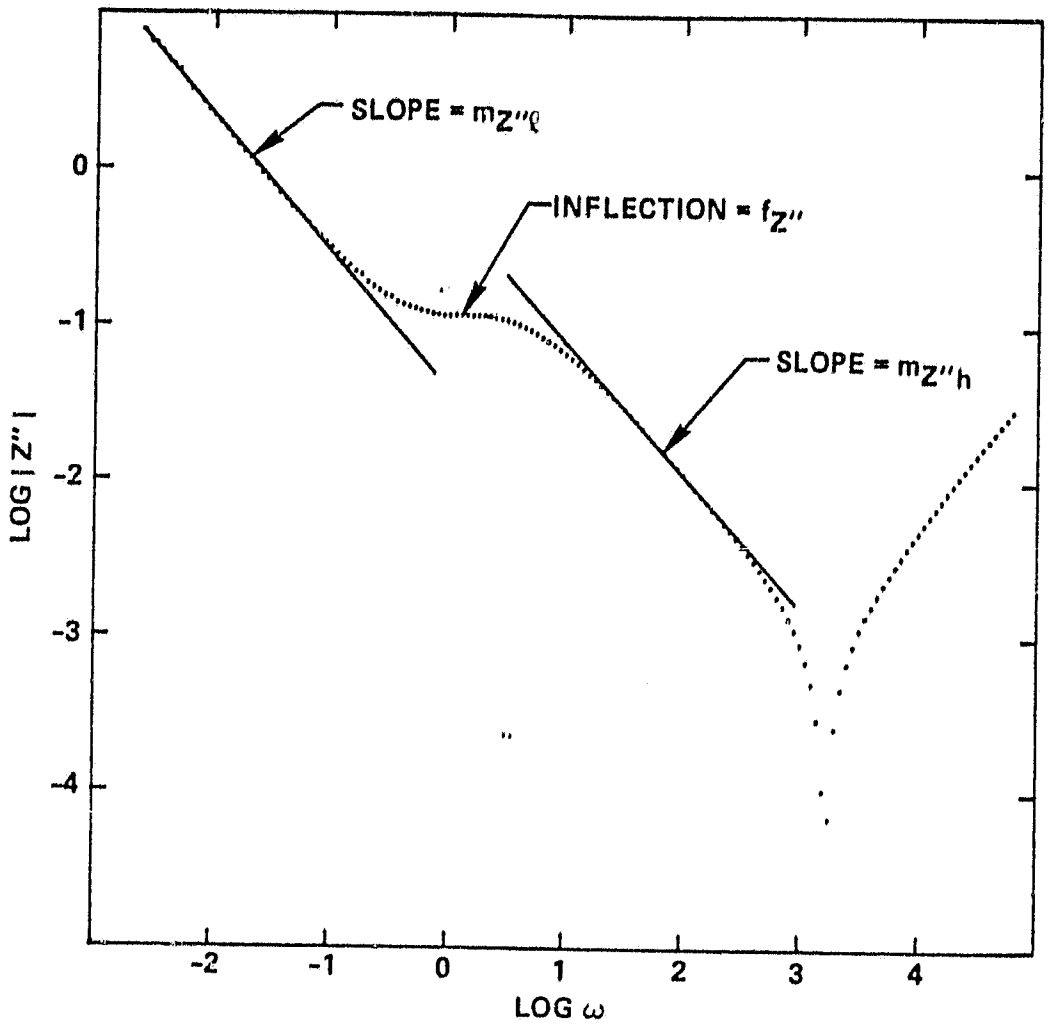

Fig. 11 Log-log plot of the imaginary impedance component vs frequency for the data given in Fig. 9.

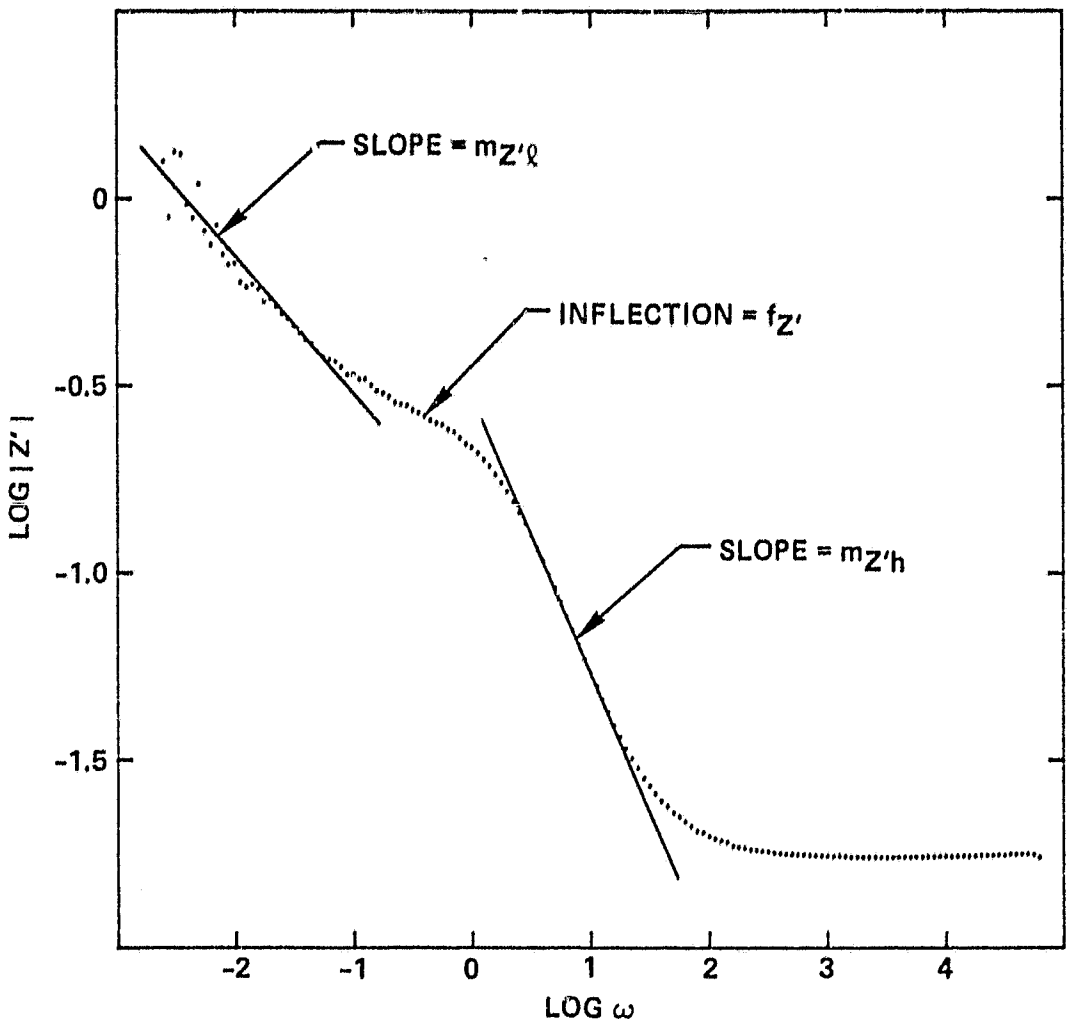

Fig. 12 Log-log plot of the real impedance component vs frequency for the data given in Fig. 9.

Table I

Dependence of W and C_{DL} for Various Ni-Cd Cells on Charge/Discharge History

Cell Number / Cycle Temperature (°C) / Depth of Discharge (%)	Charge/Discharge Cycles (Number)	W (deg)	C_p (F)
L2-59	1116	76.6	2.2
30°/35%	3457	82.4	1.7
L2-68	1957	71.6	-
30°/20%	3119	77.1	2.1
	4704	78.7	2.0
	5223	82.1	1.8
		-FAILED-	
L2-82	1132	65.6	2.0
40°/35%	2448	67.4	2.2
	4488	68.1	1.7
L2-93	378	71.6	5.2
40°/50%	1496	45.0	-
	3072	69.7	2.2
	3573	-FAILED-	
L2-95	3124	87.1	1.8
40°/50%	3351	-FAILED-	
L2-96	1561	76.6	1.9
40°/50%	3025	74.5	-
L2-102	906	69.7	1.8
30°/50%	5109	79.9	1.9
L1-68	0	79.5	8.9
35°/30%	800	80.5	4.7
	2278	81.4	5.1
L1-69	0	80.5	5.8
35°/30%	800	65.6	3.4
	2278	76.9	4.3
L1-70	0	77.4	4.2
50°/40%	800	76.3	5.8
	2126	-FAILED-	
L1-71	0	80.2	4.2
50%/40%	800	76.0	5.4

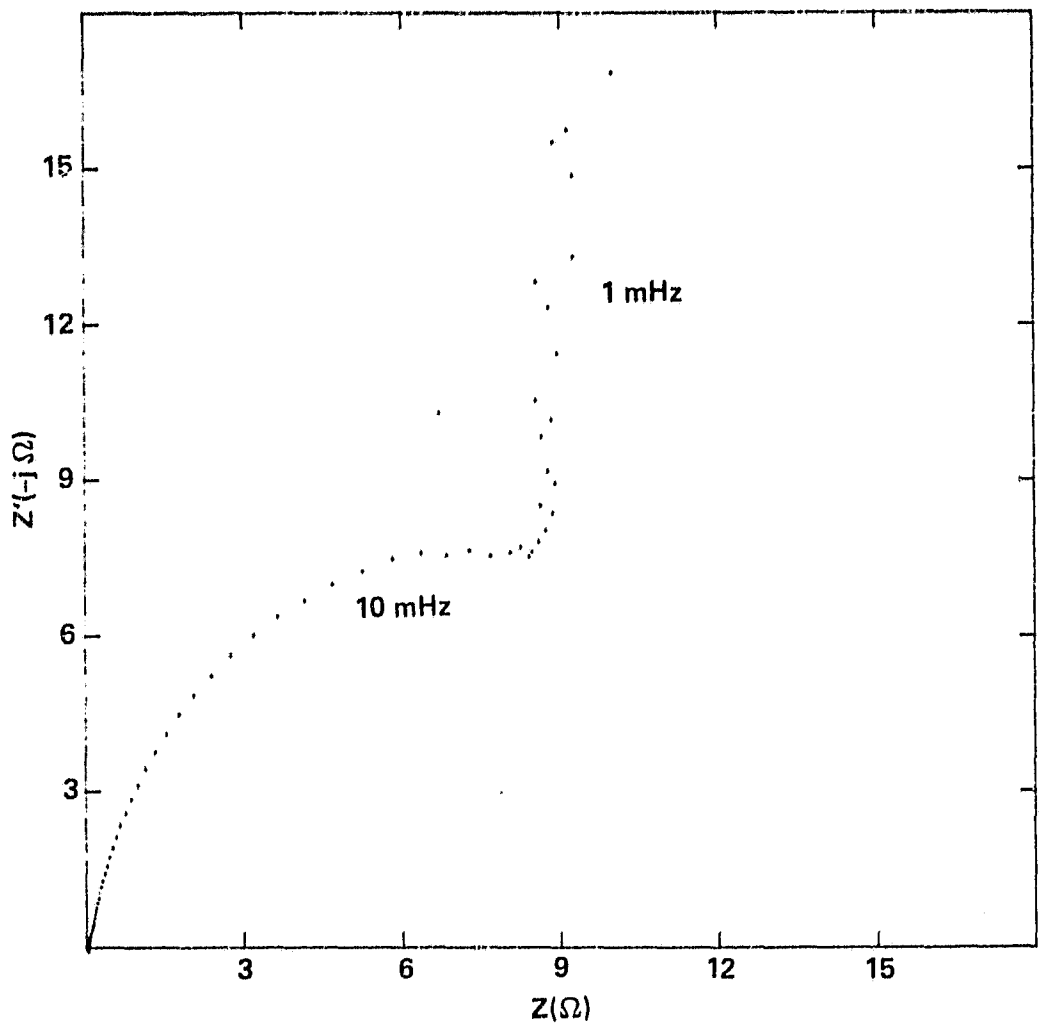

Fig. 13 Complex impedance spectrum for Ni-Cd cell L2-95 at 0.0 V after 3124 charge/discharge cycles.

A rapid falloff of W in the diffusional region may also signal cell deterioration, most probably by a different mechanism. This is evident from the complex impedance spectra for failed cells shown in Fig. 14. For the first three spectra (a-c), the low frequency diffusional response is absent, presumably because the cells have been shorted by dendrites/separator failure. For these cells, the impedance behavior is apparently dominated by double layer charging and, in cases where two semicircles are observed (Figs. 14b,c), adsorption processes. The impedance spectrum for cell L2-94 (Fig. 14d), which comprises a normal high frequency semicircle and a diffusional tail that becomes non-linear (falls off) at lower frequencies, is of particular interest. The latter behavior is typical of diffusion through a finite diffusion layer and has been observed for normal Ni-Cd cells [15]. The possibility that the deviation of Z'' from linearity in the diffusion region signals cell deterioration is supported by the preliminary data obtained for cell L2-94. Figure 15 depicts the complex impedance spectrum for this cell after 2350 cycles (1000 cycles before failure). The value of W is lower than for most cells, and the curvature in the diffusional region is greater than that observed for any other cell.

As indicated by the impedance data for L1 cells after 800 charge/discharge cycles summarized in Table II, C_p may also reflect cell deterioration. For the harsher cycle conditions (50°C, 40% depth of discharge), C_p, which also increases with cycle life for this type of cell, is considerably larger.

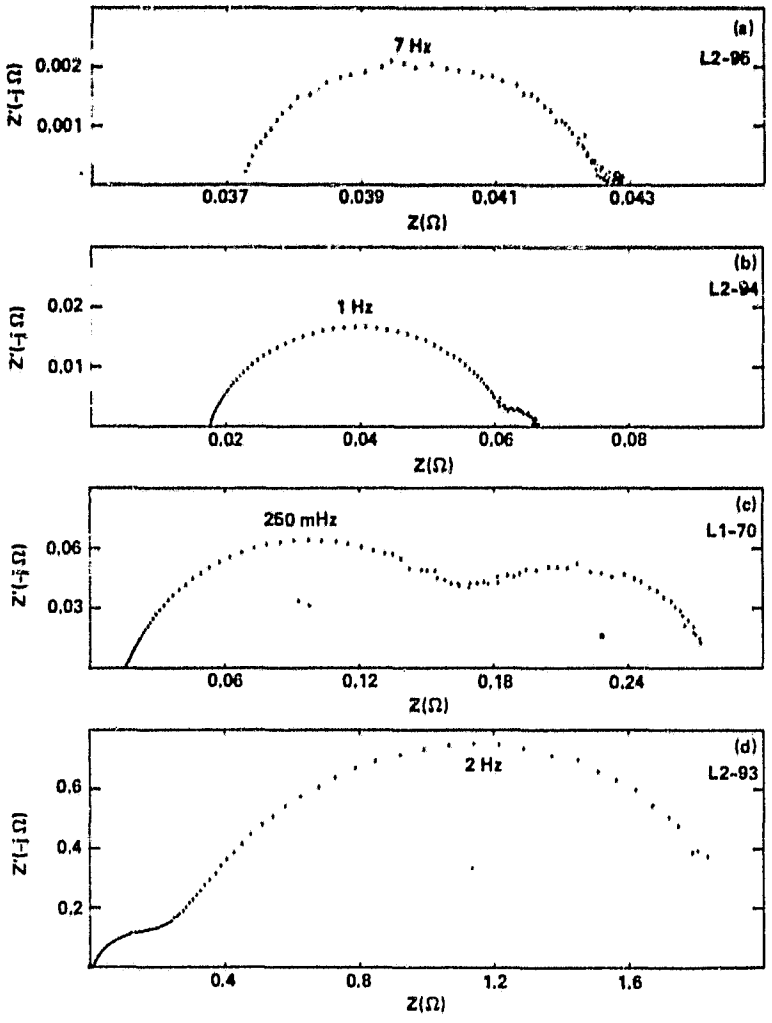

Fig. 14 Complex impedance spectra at 0.0 V for failed Ni-Cd cells: (a) L2-95; (b) L2-93; (c) L1-70; and (d) L2-94.

Table II
Dependence of C_{DL} and $m_{Z\ell}$ for L1 Cells After 800 Charge/Discharge Cycles

Cell Number	Cycle Temperature (°C)	Depth of Discharge (%)	C_p (F)	$m_{Z\ell}$
L1-68	35	30	4.7	-0.96
L1-69	35	30	3.4	-0.92
L1-70	50	40	5.8	-0.86
L1-71	50	40	5.4	-0.75

$m_{Z\ell}$ = the slope of the log Z vs log ω plot between ~ 0.4 and 5 mHz.

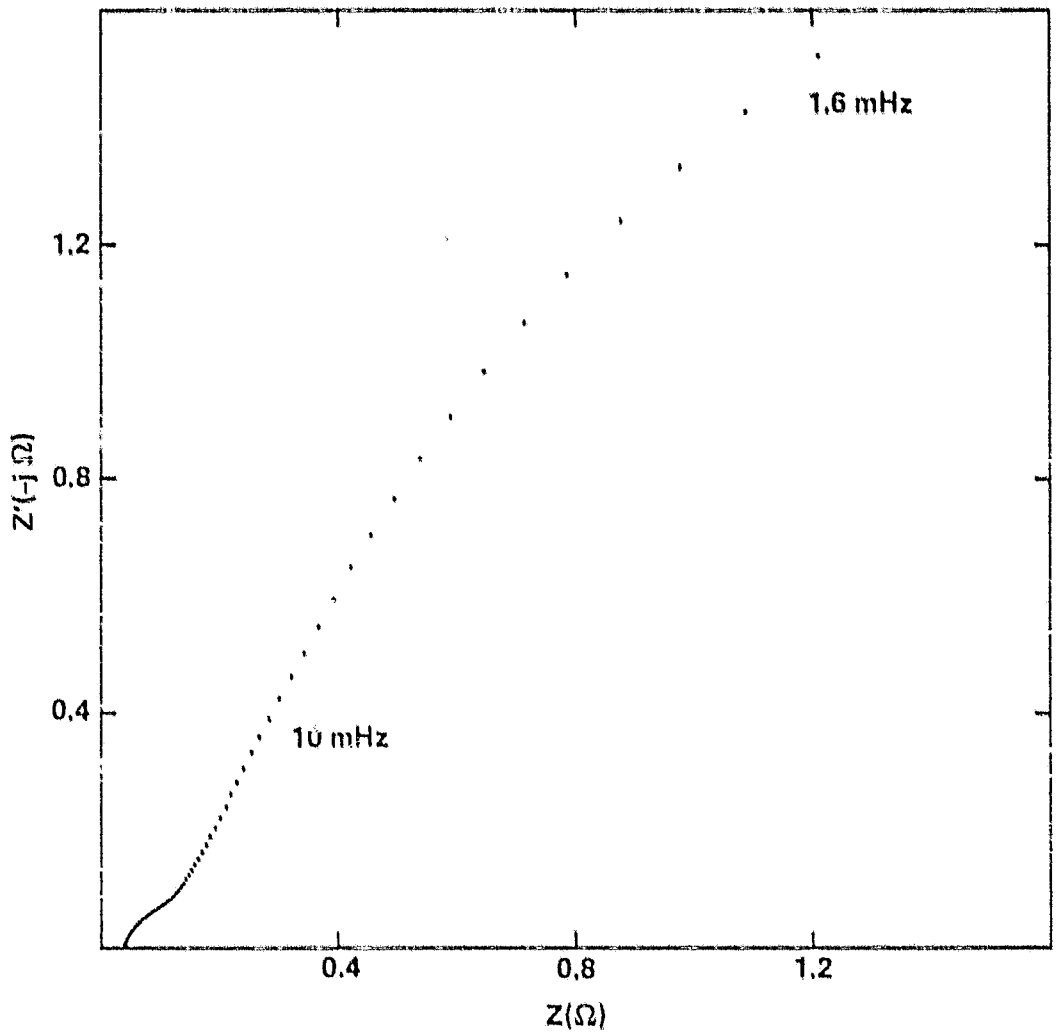

Fig. 15 Complex impedance spectrum at 0.0 V for Ni-Cd cell L2-94 after 2350 charge/discharge cycles.

3.4 State-of-Charge Determination

In view of the considerable current interest in ac impedance as a means of determining battery state of charge, data generated under the present program were evaluated for incidental relationships along these lines. It was found that increases in the state of charge are consistently reflected by a linear increase in m_{Zh}, which, as depicted in Fig. 16, is the slope of the linear portion of log Z - log ω plots between 500 and 5 mHz. Values of m_{Zh} as a function of charge state for 8 Ni-Cd cells are tabulated in Table III. Although the absolute values vary somewhat, the trend is consistent for each cell. The results indicate that low frequency impedance measurements are most promising for state of charge determinations, which is consistent with recent work involving the diffusional impedance for Ni-Cd cells [15].

Table III

Dependence of m_{Zh} on the Charge State of Various Ni-Cd Cells

State of Charge (A-hr)	m_{Zh}							
	L2-67	L2-72	L2-82	L2-88	L2-92	L2-93	L2-96	L2-102
4	-0.08	-0.062	-0.10	-0.061	-0.083	-0.083	-0.073	-0.10
8	-0.09	-0.069	-0.11	-0.069	-0.080	-	-0.10	-
12	-0.14	-0.095	-0.13	-0.095	-0.095	-0.11	-0.13	-0.18

m_{Zh} = slope of log Z - low ω plot between 500 and 5 mHz.

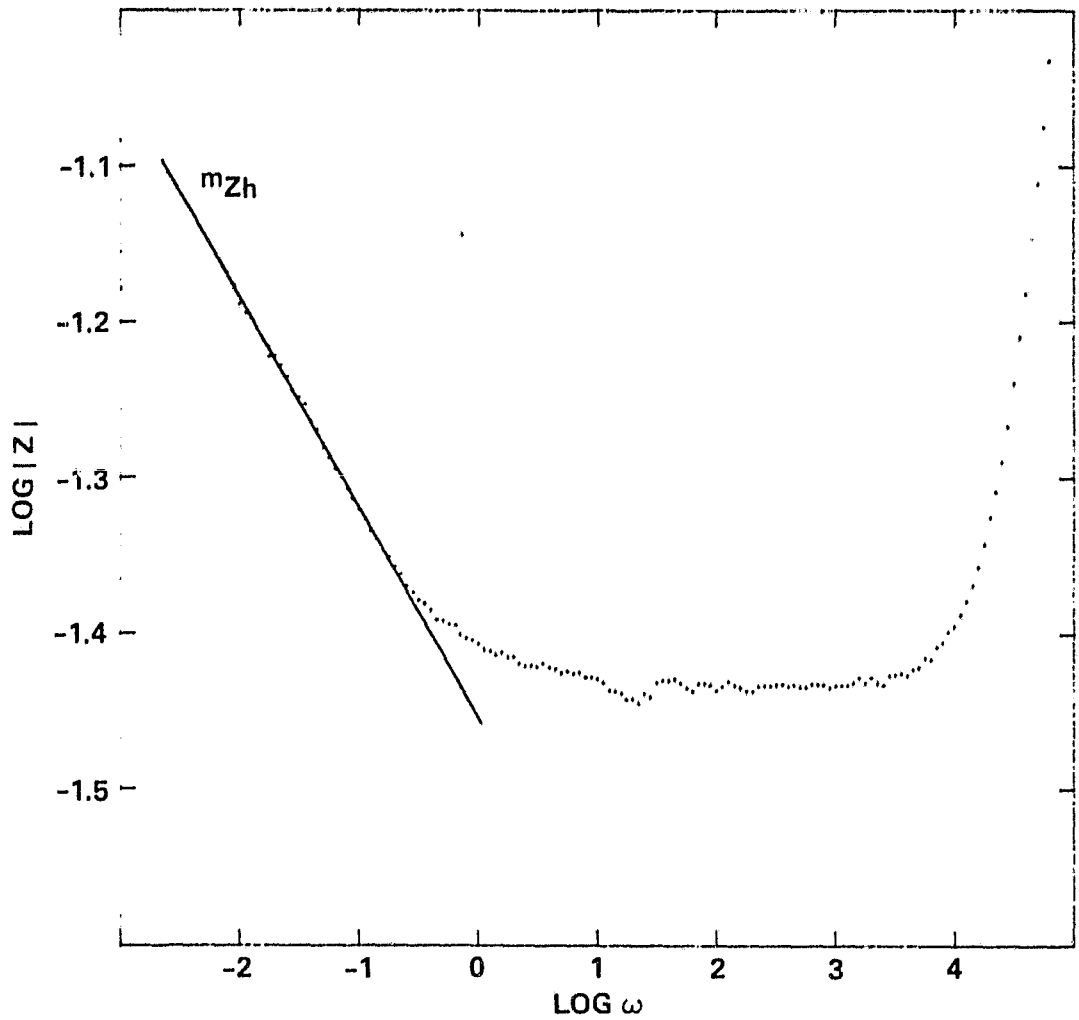

Fig. 16 Log-log plot of cell impedance vs frequency for Ni-Cd cell L2-97 at full charge.

3.5 Recommendations for Future Work

For the present program, which was of very limited scope, ac impedance techniques for use with Ni-Cd batteries have been developed and some impedance parameters which reflect cell deterioration have been identified. Unfortunately, none of the evaluated cells failed prematurely under charge/discharge cycling so that correlations between impedance characteristics and cycle life could not be verified. Thus, attainment of the long-term goal of a non-destructive method for predicting cell life will require a more comprehensive study, which would also provide valuable information for improving cell design and performance. Some guidelines for such a study, derived from the results of the present work, are outlined below.

More work is certainly warranted to investigate diffusional (low frequency) impedance parameters (measured for fully discharged cells), which have been shown to reflect battery deterioration. For example, the absolute magnitude of the Warburg angle (W) or the change in W over a few charge/discharge cycles may ultimately provide a predictive measure of the cell cycle life under some conditions. However, measurements should not be limited to the fully discharged state; this was done in the present program only because of resource limitations. One important disadvantage of measurements for discharged cells is that the impedance reflects primarily processes at the Ni electrode, whereas some important cell failure modes involve the Cd electrode.

Alternate measurement techniques, which may provide greater sensitivity (especially at the higher charge states), should also be investigated. For example, a galvanostatic method (involving a current perturbation) which was evaluated under this program warrants further attention. Figures 17 - 19 show complex impedance spectra for cell L1-67 obtained at the fully discharged state with sinusoidal current perturbations of 10, 100 and 350 mA (rms), respectively. For the 10 mA perturbation (Fig. 17), which approximates the current obtained with a 2 mV perturbation, the impedance spectra for the galvanostatic and potentiostatic approaches are equivalent. However, additional information seems to be obtained for the higher current perturbations (Figs. 18-19); three dis-

tinct spectral features (plateaux) are evident. The transient technique described by Zimmerman, et al. [15] also offers some advantages, especially for investigating diffusional processes. Study of the latter by ac impedance involves low frequency measurements that can be very time-consuming; a full impedance scan in the present work required 14 hours. The main difficulties with the transient technique, i.e., assumption of a "natural cell response" and stringent temperature control requirements, can be alleviated by utilizing the fast Fourier transform method, which represents a compromise.

A significant improvement for the potentiostatic ac impedance method could be realized if measurements could be made in the three-electrode mode. This would permit the impedance of each battery electrode to be measured separately, but would require that a third electrode, e.g., Ni/NiO (oxidized nickel wire), be built into the cell (which is sealed) at manufacture.

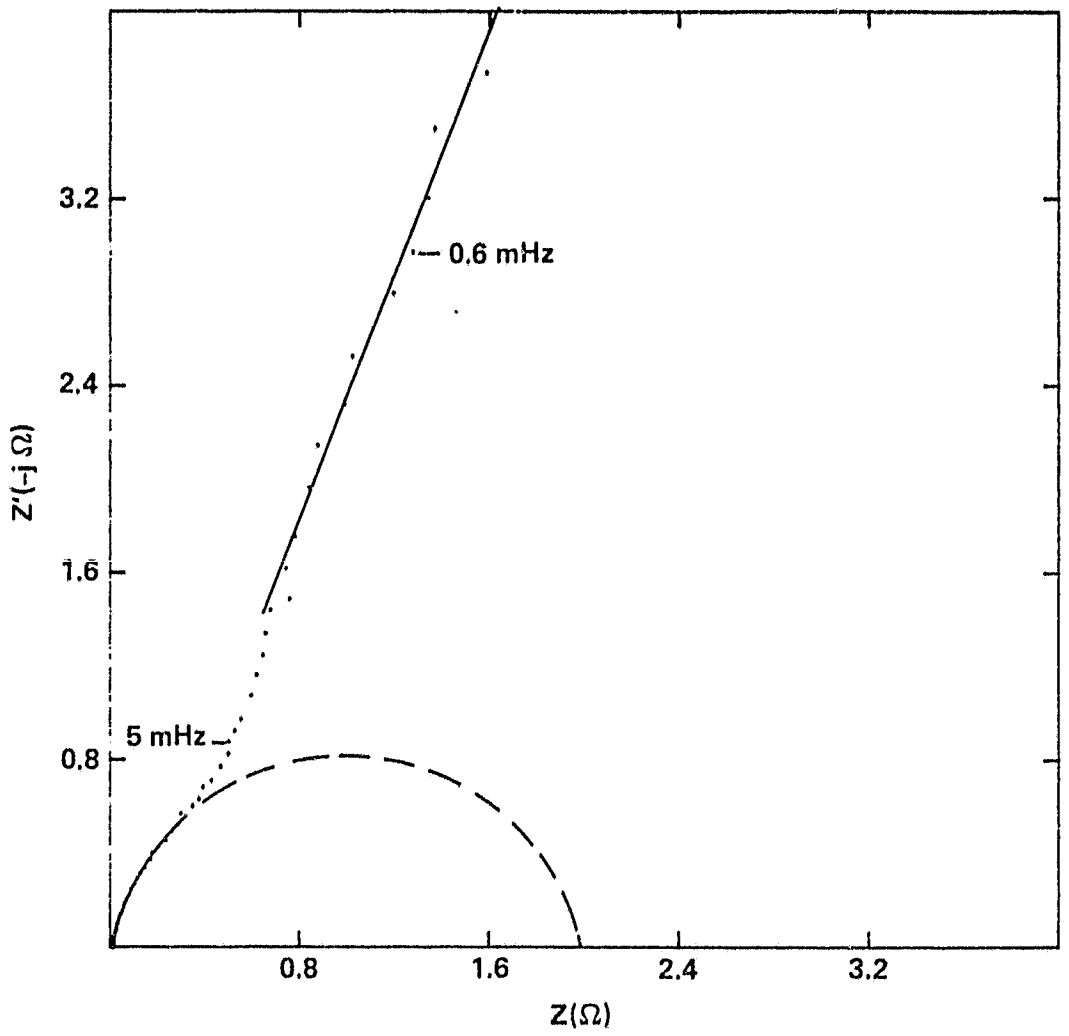

Fig. 17 Complex impedance spectrum for Ni-Cd cell L1-67 determined galvanostatically at 0.0 V using a 10 mA (rms) perturbation.

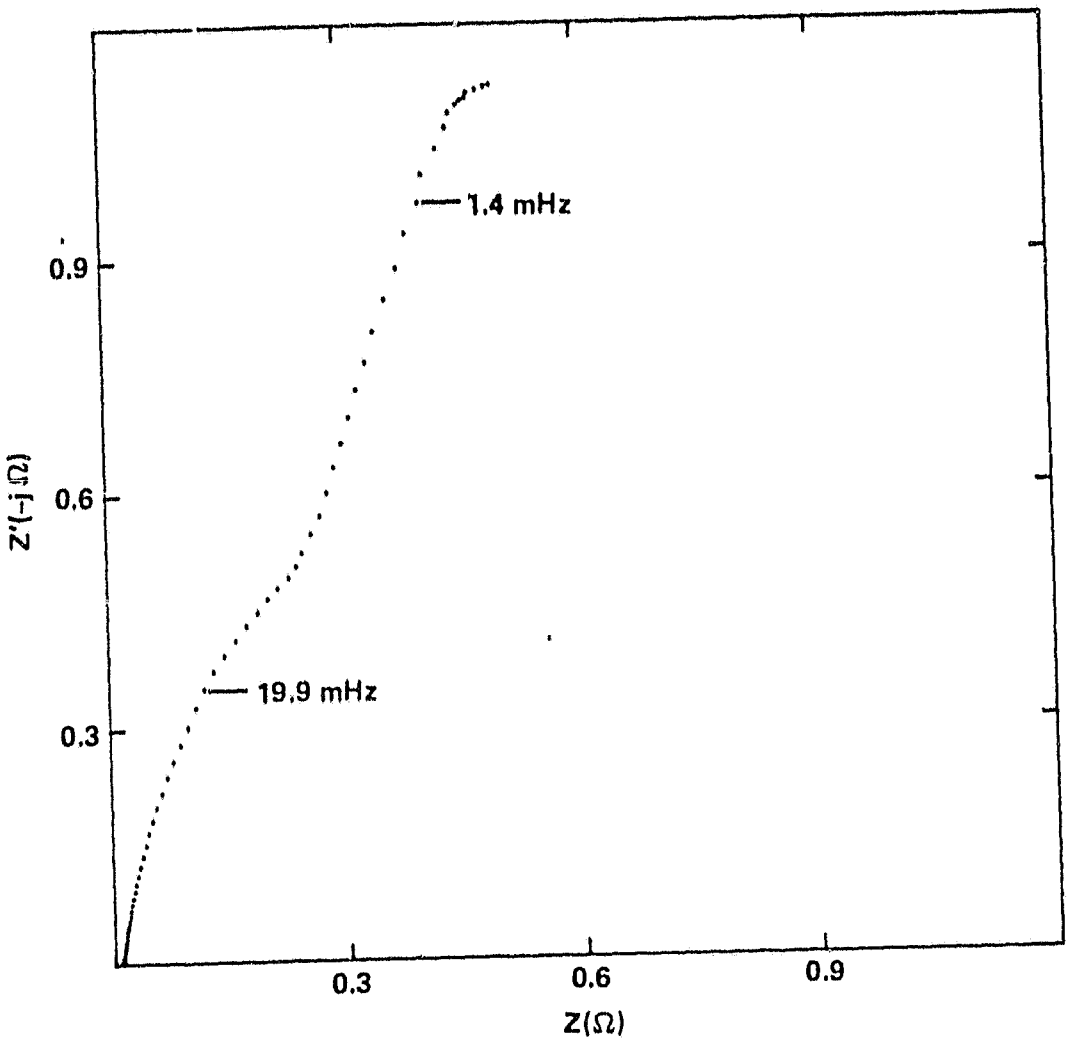

Fig. 18. Same as Fig. 17 for a 100 mA perturbation.

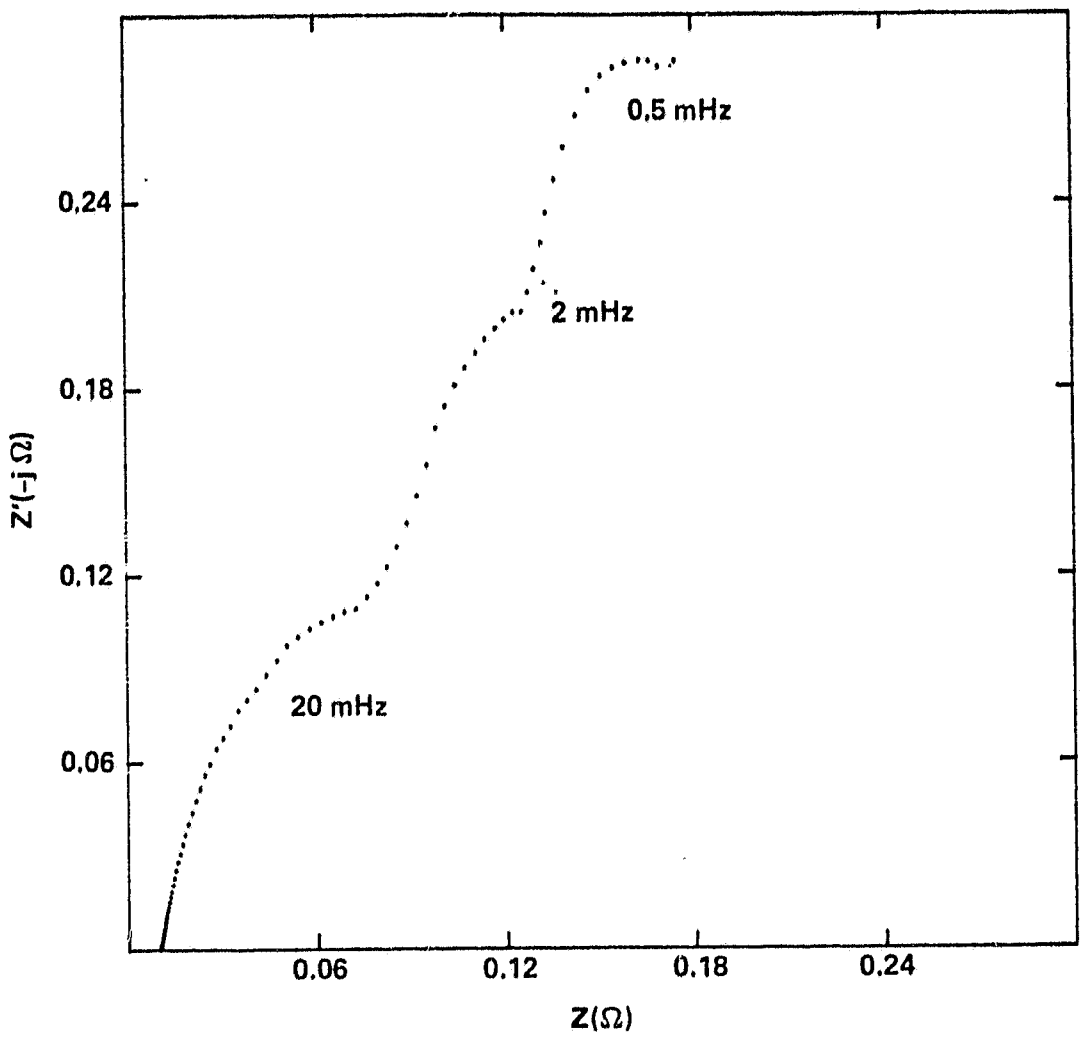

Fig. 19 Same as Fig. 17 for a 350 mA perturbation.

4.0 REFERENCES

1. R. De Levie, Adv. Electrochem. & Electrochem. Eng., Vol. 6, P. Delahay, Ed., Interscience, P. 329-397.

2. R.D. Armstrong, K. Edmonson and J.A. Lee, J. Electroanal. Chem. 63, 287 (1975).

3. H. Keiser, K.D. Beccu and M.A. Gutjahr, Electrochim. Acta 21, 539 (1976).

4. N.A. Hampson, S.A.G.R. Karunathilaka and R. Leek, J. Appl. Electrochem. 10, 3 (1980).

5. S.A.G.R. Karunathilaka, N.A. Hampson, T.P. Haas, R. Leek and T.J. Sinclair, J. Appl. Electrochem. 11, 573 (1981).

6. J.J. Winter, J.T. Breslin, R.L. Ross, H.A. Leupold and F. Rothwarf, J. Electrochem. Soc. 122, 1434 (1975).

7. S.A.G.R. Karunathilaka, N.A. Hampson, R. Leek and T.J. Sinclair, J. Appl. Electrochem. 11, 365 (1981).

8. M.L. Gopikanth and S. Sathganarayana, J. Appl. Electrochem. 9, 581 (1979).

9. S.A.G.R. Karunathilaka, N.A. Hampson, R. Leek and T.J. Sinclair, J. Appl. Electrochem. 10, 799 (1980).

10. S.A.G.R. Karunathilaka, N.A. Hampson, R. Leek and T.J. Sinclair, J. Appl. Electrochem. 10, 603 (1980).

11. S.A.G.R. Karunathilaka, N.A. Hampson, R. Leek and T.J. Sinclair, J. Appl. Electrochem. 10, 357 (1980).

12. M.L. Gopikanth and S. Sathyanarayana, J. Appl. Electrochem. 9, 369 (1979).

13. M. Keddam, Z. Stoynov and H. Takenouti, J. Appl. Electrochem. 7, 539 (1977).

14. M.R. Martinelli and A.H. Zimmerman, "Impedance Measurements on Sealed Lead-Acid Cells," Aerospace Report No. ATR-78(8114)-1, The Aerospace Corp., El Segundo, CA (1978).

15. A.H. Zimmerman, M.R. Martinelli, M.C. Janecki and C.C. Badcock, J. Electrochem. Soc. 129, 289 (1982).

16. S. Sathyanarayana, S. Venugopalan and M.L. Gopikanth, J. Appl. Electrochem. 9, 125 (1979).

17. J.A. Harrison and C.E. Small, Electrochim. Acta 26, 1555 (1981).

18. A.A. Pilla, J. Electrochem. Soc. 117, 467 (1970).

5.0 APPENDIX

Tabulation of impedance data obtained from Ni-Cd cells as described in text.

Data #	Cell #	Storage #	Test Date	Chg/ Dischg (cycles)	Hrs to 1.0 V (hr)	Charge State[1]	Perturbation Amplitude[2]

	$m_{Z'h}$	$m_{Z'l}$	$f_{Z'}$	$m_{Z''h}$	$m_{Z''l}$	$f_{Z''}$	m_{Zh}	m_{Zl}	f_Z	R_p (Ω)	ω_{max} (H_z)	C_p (f)	W (deg)	Cycle T (°C)	Cycle DoD (%)	P or G[3]
1	167	5/0/16	8/6/81	2	18.27	0.000	2									
	-0.83	-0.49	-0.80	-0.87	-0.85	0.10	-0.72	-0.86	-0.20	0.13	0.20	6.15	78.91	0	0	1
2	167	6/0/4	1/14/82	0	1.00	0.000	2									
	-0.80	-1.17	-0.70	-0.82	-1.00	0.20	-0.70	-0.85	-0.10	0.97	0.22	0.75	80.22	0	0	1
3	167	6/0/6	1/17/82	0	1.00	0.000	2									
	-0.95	-0.67	-1.50	-0.85	-0.90	-0.60	-0.88	-0.88	-0.90	0.42	0.03	15.16	75.62	0	0	1
4	167	7/0/0	6/28/82	0	1.00	0.000	2									
	-1.08	0.00	0.00	-0.85	-0.85	-1.50	-0.83	-0.82	-1.60	0.00	0.00	0.00	76.91	0	0	1
5	167	7/0/8	7/27/82	0	1.00	0.000	10									
	-1.04	-0.64	-1.80	-1.80	-0.90	-0.75	-1.60	-0.84	-0.70	0.00	0.00	0.00	73.61	0	0	0
6	167	7/0/10	7/28/82	0	1.00	0.000	10									
	-0.98	-0.70	-1.80	-0.87	-0.70	-1.20	-0.80	-0.78	-1.50	0.00	0.00	0.00	72.12	0	0	0
7	167	7/0/20	8/9/82	0	1.00	0.000	100									
	-0.90	0.68	0.00	-0.85	-0.45	-1.20	-0.82	-0.38	-1.30	0.00	0.00	0.00	71.57	0	0	0
8	167	7/0/22	8/10/82	0	1.00	0.000	100									
	-0.89	0.00	0.00	-0.85	0.00	0.00	-0.82	0.00	0.00	0.00	0.00	0.00	0.00	0	0	0
9	167	7/0/24	8/11/82	0	1.00	0.000	350									
	-0.66	0.00	0.00	-0.87	0.00	0.00	-0.63	0.00	0.00	0.00	0.00	0.00	0.00	0	0	0
10	168	5/0/6	7/31/81	2	17.27	0.000	2									
	-0.91	-0.96	-1.20	-0.85	-0.83	-0.10	-0.76	-0.76	-0.50	0.16	0.11	8.88	79.51	0	0	1
11	168	6/0/10	1/25/82	800	1.00	0.000	2									
	-0.82	-0.88	-0.70	-0.85	-0.95	0.20	-0.68	-0.96	-0.10	0.10	0.35	4.68	80.54	35	30	1
12	168	7/0/2	7/14/82	2278	0.00	0.000	2									
	-0.82	-0.62	-1.00	-0.82	-0.87	-0.10	-0.72	-0.88	-0.60	0.25	0.13	5.13	81.38	35	30	1

1. Values of 4,8,12 are in units of A hr, otherwise V or mV units apply.
2. Units are mV (rms) if potentiostatic, mA (rms) if galvanostatic.
3. P = potentiostatic control, G = galvanostatic control.

13	169	5/0/20	8/10/81	2	17.86	0.000	2									
	-0.88	-0.83	-0.90	-0.85	-0.90	0.05	-0.72	-0.90	-0.30	0.16	0.18	5.76	80.54	0	0	1
14	169	6/0/8	1/18/82	800	1.00	0.000	2									
	-0.56	-0.56	-0.40	-0.77	-0.90	0.30	-0.52	-0.92	-0.10	0.11	0.45	3.41	65.56	35	30	1
15	169	7/0/6	7/22/82	2278	0.00	0.000	2									
	-1.10	-0.40	-1.10	-0.85	-0.85	-0.50	-0.82	-0.75	-0.80	0.70	0.06	3.61	76.91	35	30	1
16	170	5/0/18	8/7/81	2	17.26	0.000	2									
	-0.80	-0.64	-0.70	-0.85	-0.90	-0.30	-0.68	-0.68	-0.10	0.08	0.45	4.36	77.74	0	0	1
17	170	5/0/22	8/11/81	2	17.26	0.000	2									
	-0.80	-0.60	-0.20	-0.80	-0.93	0.30	-0.73	-0.90	0.00	0.08	0.50	3.94	76.29	0	0	1
18	170	6/0/2	1/12/82	800	1.00	0.000	2									
	-0.93	-0.82	-0.50	-0.80	-0.90	-0.25	-0.70	-0.86	-0.10	0.12	0.22	5.85	75.26	50	40	1
19	170	7/0/4	7/15/82	2126	0.00	0.000	2									
	-0.64	0.00	0.00	-0.75	0.00	0.00	-0.58	0.00	0.00	0.15	0.25	4.24	0.00	50	40	1
20	171	5/0/8	8/3/81	2	19.28	0.000	2									
	-0.80	-0.52	-0.30	-0.80	-0.85	0.35	-0.66	-0.82	0.00	0.09	0.45	4.21	80.22	0	0	1
21	171	6/0/0	1/11/82	800	1.00	0.000	2									
	-0.80	-0.52	-0.40	-0.80	-0.85	0.35	-0.71	-0.75	0.05	0.11	0.28	5.39	75.96	50	40	1

22	259	1/0/3	7/80	0	1.00	0.000	10									
	-0.32	-0.54	-0.30	-0.75	-0.95	0.30	0.00	0.00	0.00	0.15	0.22	4.99	80.22	0	0	1
23	259	2/0/20	5/81	0	1.00	0.000	10									
	-0.42	-0.93	0.30	0.00	0.00	0.00	0.00	0.00	0.00	0.27	0.28	2.07	76.61	0	0	1
24	259	5/0/26	8/12/81	1116	10.71	0.000	5									
	-0.76	-0.52	-0.20	-0.80	-0.80	0.50	-0.68	-0.82	-0.10	0.14	0.50	2.21	76.61	30	35	1
25	259	6/1/2	5/7/82	3457	10.60	0.000	2									
	-0.70	-0.35	-0.40	-0.90	-0.85	0.15	-0.67	-0.84	-0.30	0.34	0.28	1.67	82.41	30	35	1
26	259	6/1/4	5/14/82	3457	10.60	0.000	2									
	-0.60	-0.76	-1.00	-0.90	-0.85	-0.30	-0.54	-0.75	-0.70	0.82	0.13	1.55	81.25	30	35	1
27	259	5/0/24	8/11/81	1116	10.71	0.020	5									
	-0.90	-0.53	-0.40	-0.85	-0.95	-0.40	-0.75	-0.95	-0.10	0.18	0.56	1.61	80.54	30	35	1
28	259	5/0/28	8/12/81	1116	10.71	0.100	5									
	-0.68	-0.66	-0.40	-0.75	-0.90	0.00	-0.61	-0.87	0.40	0.21	0.13	6.06	75.26	30	35	1
29	259	1/0/6	7/80	0	1.00	800.000	10									
	-0.93	0.00	0.00	0.00	0.00	0.00	0.00	0.00	0.00	0.00	0.00	0.00	85.31	0	0	1
30	259	4/0/0	5/81	0	1.00	800.000	10									
	-0.90	0.00	0.00	0.00	0.00	0.00	0.00	0.00	0.00	0.00	0.00	0.00	81.87	0	0	1
31	259	1/1/15	7/80	0	1.00	4.000	10									
	-0.16	0.00	0.00	0.00	0.00	0.00	0.00	0.00	0.00	0.00	0.00	0.00	30.11	0	0	1
32	259	1/1/17	7/80	0	1.00	8.000	10									
	-0.06	0.00	0.00	0.00	0.00	0.00	0.00	0.00	0.00	0.00	0.00	0.00	47.73	0	0	1
33	259	2/0/14	9/80	0	1.00	12.000	10									
	0.00	0.00	0.00	0.00	0.00	0.00	0.00	0.00	0.00	0.00	0.00	0.00	0.00	0	0	1
34	259	1/0/0	7/80	0	0.00	12.000	10									
	0.00	0.00	0.00	0.00	0.00	0.00	-0.08	0.00	0.00	0.00	0.00	0.00	40.36	0	0	1
35	259	6/1/8	5/17/82	3457	10.60	0.000	10									
	-0.26	-0.48	-1.50	-0.80	-0.80	0.40	-0.27	-0.92	-0.20	0.29	0.45	1.25	19.80	30	35	0
36	259	6/1/6	5/17/82	3457	10.60	0.000	10									
	0.00	0.00	0.00	-0.80	-0.90	0.50	0.00	0.00	0.00	0.00	0.00	0.00	75.26	30	35	0

37	260	3/0/12	1/81	2670	12.68	0.000	10										
	-0.81	-0.64	-1.40	0.00	0.00	0.00	0.00	0.00	0.00	2.40	0.00	23.68	64.54	20	20	1	
38	264	3/0/13	1/81	2872	9.64	0.000	10										
	-0.58	-0.70	-1.20	0.00	0.00	0.00	0.00	0.00	0.00	0.44	0.01	40.64	74.48	40	20	1	
39	267	2/0/10	9/80	1438	8.83	0.000	10										
	-1.16	0.00	0.00	0.00	0.00	0.00	-0.82	0.00	0.00	3.02	0.03	1.88	0.00	40	20	1	
40	267	2/0/0	9/80	1438	8.83	1.000	10										
	0.00	0.00	0.00	0.00	0.00	0.00	0.00	0.00	0.00	0.00	0.00	0.00	0.00	40	20	1	
41	267	1/1/11	9/80	1438	8.83	1.155	10										
	-0.40	0.00	0.00	0.00	0.00	0.00	-0.53	0.00	0.00	0.00	0.00	0.00	68.20	40	20	1	
42	267	2/1/3	9/80	1438	8.83	4.000	10										
	-0.10	0.00	0.00	0.00	0.00	0.00	-0.08	0.00	0.00	0.00	0.00	0.00	0.00	40	20	1	
43	267	2/1/5	9/80	1438	8.83	8.000	10										
	0.00	0.00	0.00	0.00	0.00	0.00	-0.10	0.00	0.00	0.00	0.00	0.00	0.00	40	20	1	
44	267	2/1/11	9/80	1438	8.83	12.000	10										
	-0.17	0.00	0.00	0.00	0.00	0.00	-0.14	0.00	0.00	0.00	0.00	0.00	0.00	40	20	1	
45	268	2/1/17	11/80	1957	12.15	0.000	10										
	-0.61	0.00	0.00	0.00	0.00	0.00	0.00	0.00	0.00	0.60	0.02	14.99	71.57	30	20	1	
46	268	2/1/21	5/81	3119	13.03	0.000	10										
	1.12	-0.46	-1.30	0.00	0.00	0.00	0.00	0.00	0.00	3.00	0.03	2.12	77.20	30	20	1	
47	268	5/1/2	12/3/81	4704	13.70	0.000	2										
	-1.22	-0.50	-1.50	-0.95	-0.85	-0.90	-0.85	-0.76	-1.20	4.60	0.02	2.04	75.96	30	20	1	
48	268	5/1/16	12/16/81	4704	13.70	0.000	2										
	-1.04	-0.42	-1.30	-0.90	-0.95	-0.50	-0.82	-0.91	-1.00	1.64	0.06	1.73	80.98	30	20	1	
49	268	6/0/36	4/16/82	5223	14.10	0.000	2										
	-1.14	-0.86	-1.20	-0.85	-0.80	-0.60	-0.85	-0.74	-0.90	2.50	0.03	1.99	0.00	30	20	1	
50	268	6/0/44	4/27/82	5223	14.10	0.000	2										
	-0.94	-0.62	-0.70	-0.85	-0.90	0.00	-0.80	-0.91	-0.40	0.45	0.20	1.77	82.09	30	20	1	

51	272	1/0/4	7/80	0	1.00	0.000	10							0	0	1
	-0.27	-0.96	0.00	0.00	0.00	0.00	0.00	0.00	0.00	0.12	1.25	1.03	80.22			
52	272	1/0/7	7/80	0	1.00	800.000	10							0	0	1
	-0.96	0.00	0.00	0.00	0.00	0.00	0.00	0.00	0.00	0.00	0.00	0.00	85.60			
53	272	1/1/16	7/80	0	1.00	4.000	10							0	0	1
	-0.10	0.00	0.00	0.00	0.00	0.00	0.00	0.00	0.00	0.00	0.00	0.00	30.96			
54	272	1/1/18	7/80	0	1.00	8.000	10							0	0	1
	-0.16	0.00	0.00	0.00	0.00	0.00	0.00	0.00	0.00	0.00	0.00	0.00	28.81			
55	272	1/0/1	7/80	0	1.00	12.000	10							0	0	1
	-0.13	0.00	0.00	0.00	0.00	0.00	0.00	0.00	0.00	0.00	0.00	0.00	19.80			
56	278	3/0/15	12/80	2438	10.70	0.000	10							20	35	1
	-1.28	0.00	0.00	-0.95	0.00	0.00	0.00	0.00	0.00	0.00	0.00	0.00	82.87			
57	278	3/0/21	12/80	2438	10.70	0.000	10							20	35	1
	-1.07	-0.86	-1.10	-0.90	-0.90	-0.50	0.00	0.00	0.00	0.00	0.83	0.00	2.55			
58	279	3/10/14	1/81	2670	5.08	0.000	10							40	35	1
	-0.50	-0.56	-0.50	0.00	0.00	0.00	0.00	0.00	0.00	0.18	0.11	7.81	76.29			
59	281	6/0/40	4/23/82	8805	0.00	0.000	2							40	35	1
	-0.86	-1.00	-0.80	-0.80	-0.80	-0.30	-0.70	-0.83	-0.60	0.55	0.06	4.59	0.00			

60	282	2/0/8	9/80	1332	5.56	0.000	10									
	-1.05	-0.45	-1.10	0.00	0.00	0.00	-0.64	-0.59	-1.00	2.50	0.03	1.99	65.56	40	35	1
61	282	2/1/22	5/81	2448	6.43	0.000	10									
	-1.01	-0.32	-1.40	-0.90	-0.70	-0.70	0.00	0.00	0.00	3.70	0.02	2.16	67.38	40	35	1
62	282	1/0/20	6/81	2448	6.43	0.000	10									
	-0.68	-0.72	-0.50	-0.85	-0.85	-0.20	-0.62	-0.80	-0.10	0.36	0.28	1.58	77.20	40	35	1
63	282	6/0/38	4/19/82	4488	8.70	0.000	2									
	-0.94	-0.29	-1.00	0.00	0.00	-0.40	-0.79	-0.65	-0.70	1.46	0.06	1.73	68.20	40	35	1
64	282	2/0/2	9/80	1332	5.56	1.000	10									
	0.00	0.00	0.00	0.00	0.00	0.00	0.00	0.00	0.00	0.00	0.00	0.00	75.96	40	35	1
65	282	1/1/9	9/80	1332	5.56	1.155	10									
	-0.55	0.00	0.00	0.00	0.00	0.00	-0.62	0.00	0.00	0.00	0.00	0.00	71.57	40	35	1
66	282	2/0/18	9/80	1332	5.56	4.000	10									
	-0.12	0.00	0.00	0.00	0.00	0.00	-0.10	0.00	0.00	0.00	0.00	0.00	0.00	40	35	1
67	282	2/1/6	9/80	1332	5.56	8.000	10									
	-0.15	0.00	0.00	0.00	0.00	0.00	0.00	0.00	0.00	0.00	0.00	0.00	0.00	40	35	1
68	282	2/1/12	9/80	1332	5.56	12.000	10									
	-0.14	0.00	0.00	0.00	0.00	0.00	-0.12	0.00	0.00	0.00	0.00	0.00	0.00	40	35	1
69	283	2/1/18	10/80	1805	9.80	0.000	10									
	-0.68	-0.81	-1.50	0.00	0.00	0.00	0.00	0.00	0.00	1.24	0.00	42.78	75.40	30	35	1

70	288	1/0/5	7/80	0	1.00	0.000	10									
	-0.57	-1.00	-0.80	-0.85	-0.95	0.00	0.00	0.00	0.00	0.22	0.13	5.68	80.54	0	0	1
71	288	2/1/20	5/81	0	1.00	0.000	10									
	-0.92	-0.36	-1.80	-0.85	-0.90	-1.40	0.00	0.00	0.00	3.10	0.00	32.09	75.96	0	0	1
72	288	3/0/23	6/81	0	1.00	0.000	10									
	-0.85	-0.58	-1.70	-0.88	0.00	0.00	0.00	0.00	0.00	0.00	0.00	0.00	74.31	0	0	1
73	288	3/0/22	6/81	0	1.00	0.000	10									
	-0.93	0.00	0.00	-0.85	0.00	0.00	0.00	0.00	0.00	0.00	0.00	0.00	57.99	0	0	1
74	288	1/0/22	6/81	0	1.00	0.000	10									
	-0.96	-0.68	-1.90	-0.85	0.00	0.00	0.00	0.00	0.00	0.00	0.00	0.00	77.47	0	0	1
75	288	1/1/14	7/80	0	1.00	4.000	10									
	-0.10	0.00	0.00	0.00	0.00	0.00	0.00	0.00	0.00	0.00	0.00	0.00	34.99	0	0	1
76	288	1/1/19	7/80	0	1.00	8.000	10									
	-0.12	0.00	0.00	0.00	0.00	0.00	0.00	0.00	0.00	0.00	0.00	0.00	21.80	0	0	1
77	288	1/0/2	7/80	0	1.00	12.000	10									
	-0.08	0.00	0.00	0.00	0.00	0.00	0.00	0.00	0.00	0.00	0.00	0.00	17.74	0	0	1
78	288	7/0/12	7/29/82	0	1.00	0.000	10									
	-1.35	-0.70	-1.80	-0.85	0.00	0.00	-0.80	0.00	0.00	0.00	0.00	0.00	65.56	0	0	0
79	288	7/0/14	8/4/82	0	1.00	0.000	10									
	0.00	0.00	0.00	-0.85	0.00	0.00	-0.80	-0.58	0.00	0.00	0.00	0.00	71.57	0	0	0
80	288	7/0/16	8/5/82	0	1.00	0.000	100									
	-0.72	0.00	0.00	-0.85	0.00	0.00	-0.74	-0.47	0.00	0.00	0.00	0.00	68.96	0	0	0
81	288	7/0/18	8/6/82	0	1.00	0.000	100									
	-0.84	0.00	0.00	-0.85	-0.60	-1.10	-0.82	-0.55	-1.10	0.00	0.00	0.00	0.00	0	0	0
82	288	7/0/26	8/18/82	0	1.00	0.000	350									
	-0.60	0.00	0.00	-0.85	0.00	0.00	-0.68	0.00	0.00	0.00	0.00	0.00	0.00	0	0	0

83	289	6/0/24	2/25/82	7208	6.40	0.000	2									
	-0.43	0.00	0.00	-0.85	-0.75	-0.30	-0.51	-0.65	-0.20	0.36	0.04	11.14	68.20	20	50	1
84	289	6/0/30	2/8/82	7208	6.40	0.000	2									
	-0.70	-0.76	-1.10	-0.80	-0.90	-0.30	-0.64	0.00	0.00	0.00	0.00	0.00	74.05	20	50	1
85	291	3/0/16	1/81	2869	7.68	0.000	10									
	-1.02	0.00	0.00	-1.00	0.00	0.00	0.00	0.00	0.00	0.00	0.00	0.00	82.87	20	50	1
86	291	1/0/23	1/81	2869	7.68	0.000	10									
	-1.32	-0.49	-1.40	-0.90	-0.85	-0.80	0.00	0.00	0.00	2.60	0.03	2.19	76.76	20	50	1
87	292	2/0/9	10/80	1436	8.52	0.000	10									
	-0.64	-0.58	-0.80	0.00	0.00	0.00	-0.56	-0.71	-0.40	0.38	0.15	2.77	77.47	20	50	1
88	292	2/0/3	10/80	1436	8.52	1.000	10									
	-0.74	0.00	0.00	0.00	0.00	0.00	0.00	0.00	0.00	0.00	0.00	0.00	45.00	20	50	1
89	292	2/0/19	10/80	1436	8.52	4.000	10									
	-0.15	0.00	0.00	0.00	0.00	0.00	-0.09	0.00	0.00	0.00	0.00	0.00	0.00	20	50	1
90	292	2/1/7	10/80	1436	8.52	8.000	10									
	-0.08	0.00	0.00	0.00	0.00	0.00	-0.08	0.00	0.00	0.00	0.00	0.00	0.00	20	50	1
91	292	2/1/13	10/80	1436	8.52	12.000	10									
	-0.10	0.00	0.00	0.00	0.00	0.00	-0.09	0.00	0.00	0.00	0.00	0.00	0.00	20	50	1

92	293	2/0/7	7/80	378	8.77	0.000	10								
	-0.54	-0.42	-1.80	0.00	0.00	0.00	-0.69	-0.76	-0.80	1.10	0.03	5.15	71.57	40	50 1
93	293	2/1/23	5/81	1496	6.17	0.000	10								
	-1.04	-1.22	-2.30	0.00	0.00	0.00	0.00	0.00	0.00	0.00	0.00	0.00	45.00	40	50 1
94	293	5/1/14	12/15/81	3072	5.50	0.000	2								
	-0.98	-0.92	-1.30	-8.00	-0.75	-0.50	-0.76	-0.75	-0.80	1.86	0.04	2.16	69.68	40	50 1
95	293	6/1/0	4/30/82	3573	1.50	0.000	10								
	-0.38	-1.20	-0.75	0.00	0.00	0.00	0.00	0.00	0.00	0.46	0.00	$$$$$	0.00	40	50 1
96	293	2/0/4	7/80	378	8.77	800.000	10								
	-1.30	0.00	0.00	0.00	0.00	0.00	-0.46	0.00	0.00	0.00	0.00	0.00	84.29	40	50 1
97	293	2/0/5	7/80	378	8.77	1.000	10								
	-0.57	0.00	0.00	0.00	0.00	0.00	-0.45	0.00	0.00	0.00	0.00	0.00	75.96	40	50 1
98	293	2/1/1	7/80	378	8.77	4.000	10								
	-0.08	0.00	0.00	0.00	0.00	0.00	-0.09	0.00	0.00	0.00	0.00	0.00	0.00	40	50 1
99	293	2/1/8	7/80	378	8.77	8.000	0								
	0.00	0.00	0.00	0.00	0.00	0.00	0.00	0.00	0.00	0.00	0.00	0.00	0.00	40	50 1
100	293	2/1/14	7/80	378	8.77	12.000	10								
	-0.12	0.00	0.00	0.00	0.00	0.00	-0.11	0.00	0.00	0.00	0.00	0.00	0.00	40	50 1
101	294	3/0/17	11/80	2350	6.06	0.000	10								
	-0.41	-0.82	-0.40	-0.75	-0.73	-0.10	0.00	0.00	0.00	0.19	0.10	8.31	63.43	40	50 1
102	294	5/0/0	7/23/81	3351	0.00	0.000	2								
	-0.78	-0.86	-0.30	-0.75	-0.75	-0.30	0.00	0.00	0.00	0.18	0.56	1.58	0.00	40	50 1
103	294	5/0/4	7/27/81	3351	0.00	0.000	2								
	-0.78	-0.66	-0.70	-0.80	-0.60	0.00	0.00	0.00	0.00	0.35	0.18	2.51	0.00	40	50 1

104	295	3/0/18	1/81	3124	6.60	0.000	10									
	-1.13	0.00	0.00	-0.90	-0.50	-1.50	0.00	0.00	0.00	14.20	0.01	1.78	77.47	40	50	1
105	295	4/0/7	6/2/81	3446	0.00	0.000	10									
	0.00	0.00	0.00	0.00	0.00	0.00	0.00	0.00	0.00	0.00	0.00	0.00	0.00	40	50	1
106	295	3/0/20	6/2/81	3446	0.00	0.000	10									
	0.00	0.00	0.00	-1.00	0.00	0.00	0.00	0.00	0.00	0.00	0.00	0.00	0.00	40	50	1
107	296	2/0/22	5/81	1561	5.68	0.000	10									
	-0.98	-0.46	-1.30	0.00	0.00	0.00	0.00	0.00	0.00	2.42	0.04	1.88	76.76	40	50	1
108	296	5/1/10	12/10/81	3025	6.75	0.000	2									
	-1.01	-0.71	-1.70	-0.80	-0.75	-1.40	-0.80	-0.82	-1.50	5.12	0.00	23.91	0.00	40	50	1
109	296	6/0/26	2/26/82	3025	6.75	0.000	2									
	-1.06	-0.78	-1.80	-0.85	-0.85	-1.35	-0.80	-0.82	-1.40	0.00	0.00	0.00	74.48	40	50	1
110	296	2/0/1	7.80	3025	6.75	1.000	10									
	-0.86	0.00	0.00	0.00	0.00	0.00	-0.74	0.00	0.00	0.00	0.00	0.00	0.00	40	50	1
111	296	1/1/10	7/80	3025	6.75	1.155	10									
	-0.53	0.00	0.00	0.00	0.00	0.00	-0.34	0.00	0.00	0.00	0.00	0.00	72.90	40	50	1
112	296	2/1/4	7/80	3025	6.75	4.000	10									
	-0.07	0.00	0.00	0.00	0.00	0.00	-0.07	0.00	0.00	0.00	0.00	0.00	0.00	40	50	1
113	296	2/1/9	7/80	3025	6.75	8.000	10									
	0.00	0.00	0.00	0.00	0.00	0.00	0.00	0.00	0.00	0.00	0.00	0.00	0.00	40	50	1
114	296	2/1/15	7/80	3025	6.75	12.000	10									
	-0.14	0.00	0.00	0.00	0.00	0.00	-0.14	0.00	0.00	0.00	0.00	0.00	0.00	40	50	1
115	296	2/0/13	7/80	3025	6.75	12.000	0									
	0.00	0.00	0.00	0.00	0.00	0.00	-0.06	0.00	0.00	0.00	0.00	0.00	0.00	40	50	1

116	297	2/1/19	11/80	2114	6.06	0.000	10									
	-1.14	0.00	0.00	0.00	0.00	0.00	0.00	0.00	0.00	0.00	0.00	0.00	78.23	30	50	1
117	297	5/1/12	12/14/81	5897	5.70	0.000	2									
	-1.20	0.00	0.00	-0.80	0.00	0.00	-0.90	0.00	0.00	0.00	0.00	0.00	0.00	30	50	1
118	297	6/0/12	1/29/82	5897	5.70	0.000	2									
	-0.74	-0.84	-0.50	-0.80	-0.75	-0.20	-0.68	-0.68	-0.10	3.10	0.20	0.26	0.00	30	50	1
119	298	3/0/19	2/81	3168	7.35	0.000	10									
	-1.12	0.00	0.00	0.00	0.00	0.00	0.00	0.00	0.00	0.00	0.00	0.00	68.20	30	50	1
120	2101	6/0/28	3/4/82	4222	6.05	0.000	2									
	-1.22	0.00	0.00	-0.90	0.00	0.00	-0.86	0.00	0.00	0.00	0.00	0.00	0.00	30	50	1
121	2102	2/0/6	8/80	906	9.33	0.000	10									
	-0.95	-0.24	-1.00	0.00	0.00	0.00	-0.81	-0.77	-0.80	1.38	0.63	0.18	69.68	30	50	1
122	2102	6/0/42	4/26/82	5109	10.00	0.000	2									
	-0.82	-0.41	-0.60	-0.85	-0.90	-0.15	-0.71	-0.84	-0.20	0.33	0.25	1.93	79.88	30	50	1
123	2102	5/1/0	12/1/82	4689	6.90	0.000	2									
	-1.18	0.00	0.00	-0.85	0.00	0.00	-0.87	0.00	0.00	0.00	0.00	0.00	0.00	30	59	1
124	2102	1/1/8	8/80	906	9.33	1.155	10									
	-0.44	0.00	0.00	0.00	0.00	0.00	-0.90	0.00	0.00	0.00	0.00	0.00	78.47	30	50	1
125	2102	2/1/2	8/80	906	9.33	4.000	10									
	-0.18	0.00	0.00	0.00	0.00	0.00	0.00	0.00	0.00	0.00	0.00	0.00	0.00	30	50	1
126	2102	2/1/16	8/80	906	9.33	12.000	10									
	-0.18	0.00	0.00	0.00	0.00	0.00	-0.18	0.00	0.00	0.00	0.00	0.00	0.00	30	50	1